



Synthesis and structure–activity relationships of 1,2,3,4-tetrahydropyrido[2,3-*b*]pyrazines as potent and selective inhibitors of the anaplastic lymphoma kinase

Karen L. Milkiewicz^{a,*}, Linda R. Weinberg^a, Mark S. Albom^a, Thelma S. Angeles^a, Mangeng Cheng^a, Arup K. Ghose^a, Renee C. Roemmele^b, Jay P. Theroff^a, Ted L. Underiner^a, Craig A. Zifcick^a, Bruce D. Dorsey^a

^a Cephalon, Inc. 145 Brandywine Parkway, West Chester, PA 19380-4245, USA

^b CPRD Cephalon Inc. 383 Phoenixville Pike, Malvern, PA 19355, USA

ARTICLE INFO

Article history:

Received 19 March 2010

Revised 23 April 2010

Accepted 25 April 2010

Available online 29 April 2010

Keywords:

Anaplastic lymphoma kinase

Kinase inhibitors

ABSTRACT

Dysregulation of the anaplastic lymphoma kinase (ALK) is implicated in a variety of cancers. A series of tetrahydropyrido[2,3-*b*]pyrazines was constructed as ring-constrained analogs of a known aminopyridine kinase scaffold. Chemistry was developed to rapidly elaborate the SAR, structural elements impacting ALK inhibitory activity were exploited, and kinase selective analogs were identified that inhibit ALK with IC_{50} values ~ 10 nM (enzyme) and ~ 150 nM (cell).

© 2010 Elsevier Ltd. All rights reserved.

1. Introduction

Anaplastic lymphoma kinase (ALK) is a cell membrane-spanning receptor tyrosine kinase which belongs to the insulin receptor subfamily. Normally, ALK has a restricted distribution in mammalian cells; the most abundant expression of ALK occurs in the neonatal brain, suggesting a possible role for ALK in early brain development.¹

ALK is implicated in the progression of several tumors. It was initially identified as a result of its involvement in anaplastic large-cell lymphomas, a subtype of non-Hodgkin lymphomas. Sixty percent of anaplastic large cell lymphomas (ALCL) contain a chromosomal mutation that generates a fusion protein comprised of nucleophosmin (NPM) and the intracellular domain of ALK.^{2,3} This mutant protein, NPM-ALK, possesses a constitutively active tyrosine kinase domain responsible for its oncogenic effect through the activation of downstream effectors.^{1,3–5} The aberrant expression of constitutively active ALK is directly implicated in the pathogenesis of ALCL and inhibition of ALK can markedly impair the growth of ALK+ lymphoma cells.^{6–11} In addition to ALCL, the constitutively activated chimeric ALK has also been implicated in approximately 60% of inflammatory myofibroblastic tumors (IMTs), a slow-growing sarcoma that primarily affects children and young adults.¹²

ALK and its putative ligand, pleiotrophin, are also overexpressed in human glioblastomas.¹³ In mouse studies, depletion of ALK decreased glioblastoma tumor growth and prolonged survival.^{14,15} In another investigative study, heritable mutations of ALK were recognized as the main cause of familial neuroblastoma in children, and the same mutations were implicated in non-inherited neuroblastomas.¹⁶ Recently, a significant report implicated that 6–7% of non-small-cell lung cancers contain a novel translocation where the echinoderm microtubule-associated protein-like 4 gene (EML4) is fused to ALK.¹⁷ Studies have shown that an ALK inhibitor may be a clinically effective treatment for non-small-cell lung cancer patients who express this translocation.¹⁸ Selective inhibition of ALK activity has verified this as a tractable target for novel therapies for several human cancers.¹⁹

ALK inhibitors such as pyrazolo[3,4-*c*]isoquinoline **A**,²⁰ 5-arylpyridone-carboxamide **B**,²¹ thiazole **C**,²² diaminopyrimidine **D**²³ and 2-aminopyridines^{24–26} **E** (PF-2341066, Fig. 1) have been reported for the treatment of both hematopoietic and non-hematopoietic malignancies. The latter compound is an orally bioavailable, dual c-Met/ALK inhibitor with a reported ALK cellular IC_{50} value of 24 nM and is currently in phase 3 clinical trials targeting ALK.²⁷

Constraining the conformational flexibility of ligands can facilitate binding by decreasing the entropic cost required to adopt a preferred binding orientation. For ATP-competitive kinase inhibitor scaffolds, this is particularly desirable, as the ATP binding pocket typically favors a planar hinge-binding motif with distinct spatial requirements for additional electrostatic interactions.²⁸ Such a strategy was employed to interrogate the structural requirements

* Corresponding author. Tel.: +1 610 738 6823; fax: +1 610 344 0065.
E-mail address: kmilkiew@cephalon.com (K.L. Milkiewicz).

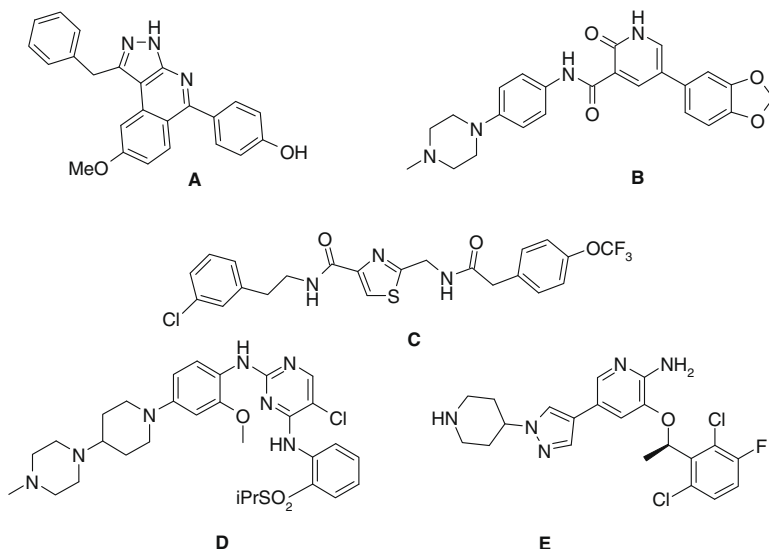


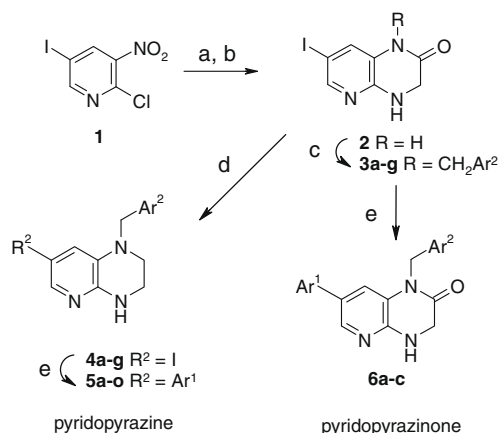
Figure 1. Reported ALK inhibitors.

of ALK inhibition after constraining the 2-aminopyridine scaffold into a fused ring system (e.g., a tetrahydropyridopyrazine scaffold, Fig. 2). This paper describes the synthesis of two distinct constrained aminopyridine scaffolds, the 1,2,3,4-tetrahydropyrido[2,3-*b*]pyrazines (THPPs) and the 1,2,3,4-tetrahydro-[1,8]naphthyridines (THNTs) and the structure–activity relationships with regards to the pendant aryl groups (Ar_1 and Ar_2) and the nature of the linker (A-L) (Fig. 2).

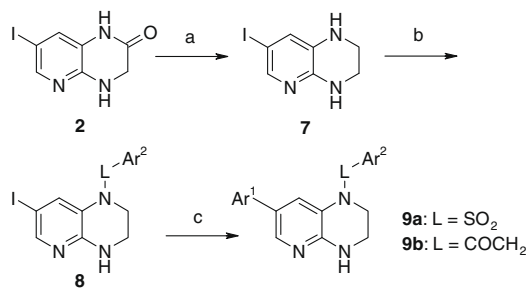
2. Chemistry

The THPP/oxo-THPP scaffold was prepared as outlined in Scheme 1. Coupling of pyridine **1**³⁰ with glycine ethyl ester afforded an aminopyridine which was subsequently reduced and cyclized in one pot to afford oxo-THPP **2**. Compound **2** was selectively alkylated with substituted benzyl bromides to form **3a–g** which were subsequently subjected to a Suzuki–Miyaura coupling to afford analogs **6a–c**. Alternatively, the alkylated oxo-THPP analogs **3a–g** were reduced to the THPPs with DIBAL prior to Suzuki–Miyaura coupling which in turn afforded compounds **5a–o**. Similarly, THPPs with amide and sulfonamide linkers were synthesized from oxo-THPP **2** in three steps as outlined in Scheme 2.

The synthesis of the phenoxy linked THNT scaffold is outlined in Scheme 3. Reduction of 7-bromo-2,3-dihydro-1*H*-[1,8]naphthyridin-4-one³¹ **10** with sodium borohydride afforded alcohol **11** which was then converted to regioisomer **12** by a debromination–bromination procedure; thus, metal-halogen exchange fol-



Scheme 1. Synthesis of the THPP/oxo-THPP analogs **5** and **6**. Reagents and conditions: (a) glycine ethyl ester HCl, EtOH, TEA, 80 °C; (b) $SnCl_2 \cdot 2H_2O$, EtOH, 80 °C; (c) NaH, Ar^2CH_2Br , DMF; (d) DIBAL, CH_2Cl_2 , –78 °C to rt; (e) aryl boronate, K_2CO_3 , $PdCl_2(PPh_3)_2$, THF/water, 70 °C.



Scheme 2. Synthesis of sulfonamide and amide linked THPPs. Reagents and notes: (a) DIBAL, CH_2Cl_2 , –78 °C to rt; (b) Ar^2SO_2Cl or Ar^2COCl , pyridine; (c) $Ar^1B(OH)_2$, K_2CO_3 , $PdCl_2(PPh_3)_2$, THF/water, 70 °C.

lowed by a MeOH quench gave non-brominated intermediate that was brominated at C6 with NBS to afford **12**. Suzuki coupling followed by the ether forming Mitsunobu reaction afforded the desired phenoxy THNT analogs **14**.

Scheme 4 outlines the synthesis of the benzyl THNT scaffold **19**. Ketone **10** was converted to vinyl iodide **15** by means of the Takai reaction,³² and was subsequently converted to **16** by Suzuki

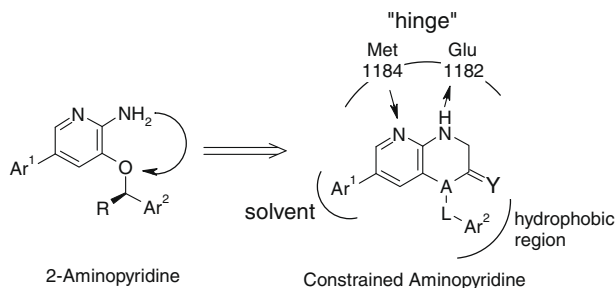
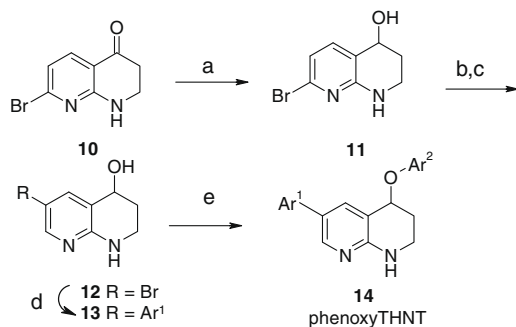
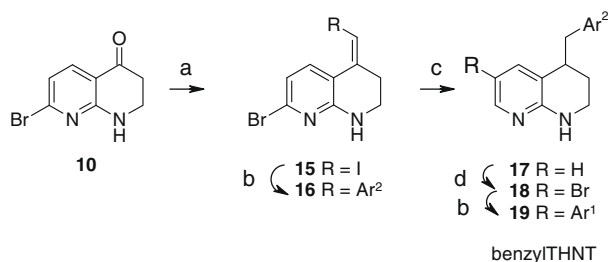


Figure 2. Strategy to constrain the aminopyridine scaffold. A-L = N- CH_2 : THPP/oxo-THPP; A-L = CH- CH_2 : benzyl THNT; A-L = CH-O: phenoxy THNT.



Scheme 3. Synthesis of the phenoxy linked THNT analogs. Reagents and notes: (a) NaBH₄, MeOH; (b) *n*-BuLi, then MeOH; (c) NBS, CH₂Cl₂/AcOH; (d) Ar¹B(OH)₂, K₂CO₃, PdCl₂(PPh₃)₂, THF/water, 70 °C; (e) Ar²OH, DEAD, Ph₃P, CH₂Cl₂, rt.



Scheme 4. Synthesis of the benzyl linked THNT analogs. Reagents and notes: (a) CrCl₂, CHI₃, THF; (b) Ar²B(OH)₂, Na₂CO₃, Pd(PPh₃)₄, toluene/EtOH/water, 90 °C; (c) Pd/C, H₂, MeOH; (d) NBS, CH₂Cl₂, AcOH.

coupling with arylboronates. Subsequent hydrogenation reduced both the alkene and the C7-Br to afford the core benzyl THNT **17**. Bromination of **17** with NBS and a second Suzuki coupling afforded the desired benzyl THNT **19**.

3. Results

Four areas of the constrained aminopyridine scaffold were explored, including Ar¹, Ar², the core scaffold itself (varying A and Y), and the linker (L) (Fig. 2). An initial series of THPPs (**5**) and oxo-THPPs (**6**) were synthesized with Ar₁ as a phenyl pyrrolomethylpyrrolidinyl amide. This initial Ar₁ was chosen because it was found to impart activity in the aminopyridine series.²⁴ The SAR for the target kinase, ALK, is summarized in Table 1.

As can be seen from the results in Table 1, ALK inhibitory activity was at least 10-fold weaker for oxo-THPP analogs (**6**, Y = O) compared with THPP analogs (**5**, Y = H₂). Also, ALK inhibition was greater for analogs bearing halogenated rather than unsubstituted benzyl groups (e.g., **5b–c**, vs **5a** and **6b–c** vs **6a**).

Another Ar¹ group that proved active in the aminopyridine series²⁴ was methylpiperazinylpyridine, and a series of THPPs and THNTs were prepared with this group held constant while varying the nature of linker (L). The SAR summarized in Table 2 shows that the nature of the linker (A-L) proved a critical determinant of potency. Sulfonamide **9a** (A-L = N-SO₂, ALK IC₅₀ = 465 nM) was 14-fold less active than benzyl amine **5d** (ALK IC₅₀ = 33 nM). Amide analog **9b** (A-L = N-COCH₂) was devoid of ALK activity. In the THNT series, both the phenoxy analog **14** (A-L = CH-O) and the benzyl analog **19** (A-L = CH-CH₂) had substantially lower potency than the corresponding analogs in the THPP series (**5h** and **5d**, respectively).

As noted earlier, analogs with halogenated aryl rings had lower ALK IC₅₀ values than unsubstituted phenyl rings (e.g., **5b–c** and **6b–c** vs **5a** and **6a**, Table 1). The nature of the halogenation pattern on

Table 1
ALK enzyme potency of oxo-THPP versus THPP analogs

Compound #	Ar ²	Y	ALK enzyme IC ₅₀ ^a
5a 6a		H ₂ O	256 >10,000
5b 6b		H ₂ O	27 278
5c 6c		H ₂ O	15 145

^a IC₅₀ values in nM reported as the average of at least two separate determinations.

the benzyl ring of the THPP influenced the potency of the series. Compounds with 2,5-disubstitution and 2,3,6-trisubstitution had the highest activity compared to the unsubstituted phenyl. Substituents as large as a trifluoromethyl were tolerated in the 2 position (**5e**), whereas a trifluoromethyl substituent was not tolerated in the 5 position (**5f**).

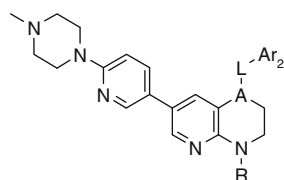
Keeping Ar² = 2-trifluoromethyl-5-chlorobenzyl, a series of THPPs varying only in the C-7 substituent was prepared. The SAR is summarized in Table 3. Whereas 4-phenylcarboxylic ester (**5i**) or acid (**5j**) analogs showed weak ALK inhibitory activity, a variety of 4-phenylcarboxamide (**5k–m**) and 2-aminopyridin-4-yl (**5n–o**) analogs demonstrated comparatively higher inhibitory activity. Phenylcarboxamides bearing a basic amine had as much as 10-fold lower ALK IC₅₀ values than those with non-ionizable functionality (**5m** vs **5k**, for example). On the other hand, modulating the basicity of the C7-piperazinylpyridine series, had less of an effect on ALK IC₅₀ values (**5e** and **5n** vs **5o**).

Compounds with IC₅₀ values of less than 50 nM in the isolated enzyme assay were tested for their ability to inhibit ALK phosphorylation in Karpas-299 cells. Table 3 shows ALK cellular IC₅₀ values for selected compounds ranged from 150 to 450 nM.

The kinase selectivity of the more potent ALK inhibitors was assessed using Ambit Bioscience's KINOMEScan™ technology and is expressed as an S(90) value; the fraction of kinases inhibited greater than 90% when screened at 1 μM across a panel of 250–400 kinases.³³ This panel includes representative kinases from all the known kinase families. The THPP analogs demonstrated a high degree of selectivity; even the least selective of them only had an S(90) value of 0.051, indicating that at 1 μM, only 5% of the evaluated kinases were inhibited greater than 90%. Percent inhibition values against individual kinases are included in the Supplementary data.

The common kinases inhibited include ALK, ARK5, CSF-1R, DCAMKL1-3, EPHB4, FAK, FLT3, JAK2, JAK3, KIT, LTK, MET, ROS1, SNARK, and TNK2. The majority of these kinases are tyrosine kinases. ALK shares a sequence homology with LTK and ROS, and the activity against MET can be anticipated, as the aminopyridine PF-2341066 is a known dual ALK/Met inhibitor. Because ALK belongs to the insulin receptor superfamily, inhibiting the insulin receptor was a potential liability which could lead to dysregulation

Table 2
Influence of the aryl linker and substitution pattern on ALK enzyme potency



Compound #	A	L	R	Ar ²	ALK enzyme IC ₅₀ ^a	S(90) ^b
5d	N	CH ₂	H		33	0.012
5e	N	CH ₂	H		10	0.022
5f	N	CH ₂	H		506	NT ^c
5g	N	CH ₂	H		11	0.020
5h	N	CH ₂	H		11	0.025
9a	N	SO ₂	H		465	NT
9b	N	COCH ₂	H		>10,000	NT
14	CH	O	H		>10,000	NT
19	CH	CH ₂	H		1538	NT
20	N	CH ₂	CH ₃		>3000	NT

^a IC₅₀ values in nM reported as the average of at least two separate determinations.

^b Kinase selectivity was determined using the Ambit Bioscience KINOMEScan™ technology, and is expressed as S(90), the fraction of kinases inhibited >90% when screened at 1 μM across a panel of 250–400 kinases.

^c NT = not tested.

of normal metabolic pathways. To confirm the lack of IR activity seen in the Ambit scan, compounds with an ALK IC₅₀ <100 nM were evaluated and were found to be inactive (>3000 nM) against IR.

3.1. Computational chemistry and discussion of results

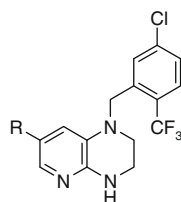
Docked poses of 2-aminopyridine **E** and THPP analog **5d** into ALK homology models²⁹ indicated that these related scaffolds shared a high level of conformational overlap (Fig. 3). In general, the predicted binding mode anchored the ligands into the ATP binding pocket using the pyridine nitrogen to accept a hydrogen bond from the gatekeeper+3 (gk+3) residue (Met-1184) and the adjacent amino group to donate a hydrogen bond to the gk+1 residue (Glu-1182). The pendant aryl group (Ar²) was directed into a

hydrophobic region on the bottom of the ATP pocket and the substituent Ar¹ pointed out towards solvent exposed space.

The Glide XP score and Embrace ΔE for ligand–protein complex formation were computed for all ligands. It was possible to interpret the SAR in the context of these docking poses. As depicted in Figures 2 and 3, N4-H and N5 (in the THPP) make putative H-bonds with residues in ALK (Glu-1182 and Met-1184). Consistent with this model is the drop in inhibitory activity going from N4-H analog **5g** (ALK IC₅₀ = 11) to N4-Me analog **20** (ALK IC₅₀ >3000 nM Table 2).

Comparing compounds **5a–c** versus **6a–c** a major decrease in activity is observed when a hydrophilic C=O is placed in a fairly hydrophobic region (Fig. 4 arrow). The salt bridge Lys-35 is too distant (~7 Å) to have any positive compensatory influence. The

Table 3
Influence of the 7-aryl substituent on ALK binding affinity



Compound #	R	ALK enzyme IC ₅₀ ^a	Karpas-299 cell IC ₅₀ ^a	S(90)
5e		9	200	0.022
5i		>3000	NT	NT
5j		1302	NT	0.023
5k		121	NT	0.008
5l		40	450	0.019
5m		10	250	0.051
5n		10	150	0.067
5o		17	250	0.027

^a IC₅₀ values in nM reported as the average of at least two separate determinations.

halogens on the benzyl group enhanced binding by their ability to interact with the salt bridge Lys³⁴ as well as by the hydrophobic interactions with residues like Leu-141 at the bottom of the ATP binding site (Fig. 4).

4. Conclusion

Constraining the known aminopyridine kinase scaffold into a THPP ring system proved a viable strategy to afford potent ALK inhibitors. The nature of the linker (A-L, Fig. 2) was found to be a critical determinant for activity, with the THPP scaffold providing far greater inhibition than the oxo-THPP and THNT scaffolds. These compounds also inhibited ALK phosphorylation in Karpas-299 cells with IC₅₀ values ranging from 100 to 450 nM. Additionally, the constrained aminopyridine scaffold provided a means to afford potent ALK inhibitors while maintaining selectivity over IR in particular and over other kinases in general. Computational modeling was consistent with the empirical SAR and could be used to guide further medicinal chemistry efforts.

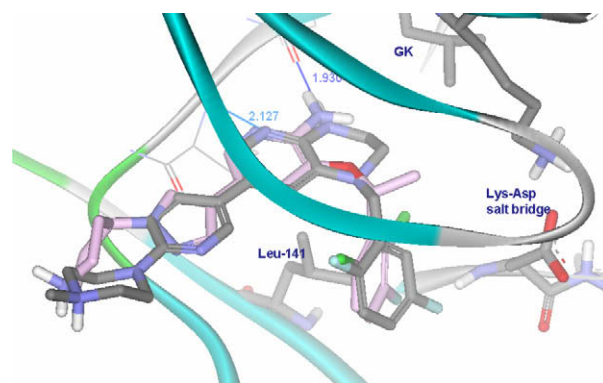


Figure 3. The basic binding mode of the constrained 2-aminopyridine (**5d**), as derived by Glide, along with the aligned ligand from the PDB file 2WGJ (PF-2341066) (light pink). This binding mode was consistent with the empirical rules for ligand binding mode prediction derived from the protein data bank kinase structures. Here the amino-NH was bound to the gk+1 residue and the pyridine-N was bound to the gk+3 residue. The gate keeper in the current model was Leu-81.

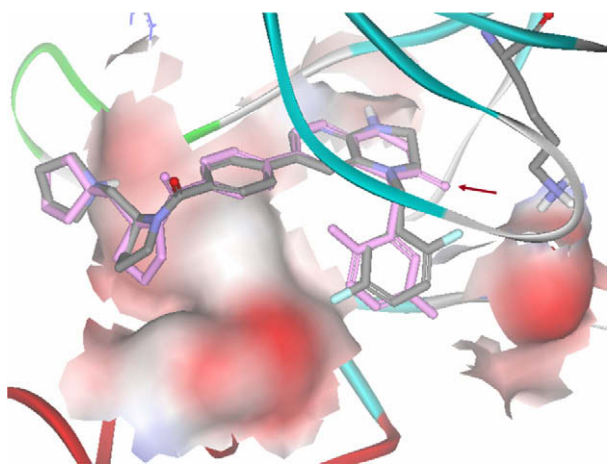


Figure 4. Comparison of the binding mode of the THPP **5c** (atom color) versus the oxo-THPP **6c** (pink). Gray surface represents nonpolar surface, red represents negatively charged surface and blue represents positively charged surface. The oxo-THPP C=O can be seen pointing into a hydrophobic region.

5. Experimental

All reagents and solvents were obtained from commercial sources and used as received. ^1H NMR spectra were obtained on a Bruker Avance at 400 MHz in the solvent indicated with tetramethylsilane as an internal standard. Analytical HPLC was run using a Zorbax RX-C8, 5×150 mm column eluting with a mixture of acetonitrile and water containing 0.1% trifluoroacetic acid with a gradient of 10–100%. LC-MS results were obtained on a Bruker Esquire 200 ion trap. Automated column chromatography was performed on a CombiFlash Companion (ISCO, Inc.). Melting points were taken on a Mel-Temp apparatus and are uncorrected.

5.1. Homology modeling

A homology model of ALK was built from the kinase domain (1116–1392) of ALK_Human sequence (Swiss-Prot entry Q9UM73). The Prime module of Schrodinger (www.schrodinger.com) software was used for this purpose. A single DFG-in homology model was built from insulin like growth factor receptor (IGF1R) structures. Prime blast search identified IGF1R having the highest sequence identity and homology with ALK. The sequence alignment was provided in the [Supplementary data](#). These observations were consistent with the finding of Gunby et al.³⁵

5.2. Docking study

The essential steps in the current docking experiment are summarized below:

- (i) Build 3D structures using LigPrep;
- (ii) Calculate electrostatic potential fitted charge using 6-31G/B3LYP in Jaguar;
- (iii) 1000 steps mixed-torsional/low-mode conformational search in MacroModel using the supplied atomic charges and implicit water solvent model;
- (iv) Glide/XP docking to keep top 10 binding poses;
- (v) Selection of the binding mode using our knowledge based approach;²⁸
- (vi) Embrace minimization of the ligand-protein complex.

Most of these modules are available in the Schrodinger molecular modeling package.

5.3. ALK kinase assay

Compounds were tested for their ability to inhibit the kinase activity of baculovirus-expressed ALK using a modification of the ELISA protocol reported for trkA.³⁶ Phosphorylation of the substrate, phospholipase C-gamma (PLC- γ) generated as a fusion protein with glutathione S-transferase (GST),³⁷ was detected with a europium-labeled anti-phosphotyrosine antibody and measured by time-resolved fluorescence (TRF). Briefly, each 96-well plate was coated with 100 μl /well of 10 $\mu\text{g}/\text{ml}$ substrate (phospholipase C- γ) in Tris-buffered saline (TBS). The assay mixture (total volume = 100 μl /well) consisting of 20 mM HEPES (pH 7.2), 1 μM ATP (K_m level), 5 mM MnCl_2 , 0.1% BSA, 2.5% DMSO, and various concentrations of test compound was then added to the assay plate. The reaction was initiated by adding enzyme (30 ng/ml ALK) and was allowed to proceed at 37 $^\circ\text{C}$ for 15 min. Detection of the phosphorylated product was performed by adding 100 μl /well of Eu-N1 labeled PT66 antibody (Perkin Elmer # AD0041). Incubation at 37 $^\circ\text{C}$ then proceeded for 1 h, followed by addition of 100 μl enhancement solution (Wallac #1244-105). The plate was gently agitated and after 30 min, the fluorescence of the resulting solution was measured using the EnVision 2100 (or 2102) multilabel plate reader (Perkin Elmer).

Data analysis was performed using ActivityBase (IDBS, Guilford, UK). IC_{50} values were calculated by plotting percent inhibition versus \log_{10} of the concentration of compound and fitting to the non-linear regression sigmoidal dose-response (variable slope) equation in XLFit (IDBS, Guilford, UK).

5.4. Cellular ALK phosphorylation measured by immunoblotting and ELISA assays

Immunoblotting of phospho-NPM-ALK and total NPM-ALK from cell lysates was carried out according to the protocols provided by the antibody suppliers. In brief, after treatment of compounds, cells were lysed in Frak lysis buffer [10 mM Tris, pH 7.5, 1% Triton X-100, 50 mM sodium chloride, 20 mM sodium fluoride, 2 mM sodium pyrophosphate, 0.1% BSA, plus freshly prepared 1 mM activated sodium vanadate, 1 mM DTT, and 1 mM PMSF, protease inhibitors cocktail III (1:100 dilution)]. After brief sonication, the lysates were cleared by centrifugation, mixed with sample buffer and subjected to SDS-PAGE. Following transfer to membranes, the membranes were blotted with either rabbit phospho-NPM-ALK(Y664) (Cat# 3341) or ALK antibody (Cat# 3342) from Cell Signaling Technology (Beverly, MA), and then the HRP-conjugated goat anti-rabbit antibodies (Santa Cruz, CA) after washed in TBS/0.2% Tween-20. The protein bands were visualized with Enhanced Chemiluminescence and quantitated with gel-pro analyzer.

To measure ALK tyrosine phosphorylation in cells with an ELISA assay, fluoronunc plates (Cat# 437796, Nalge Nunc, Rochester, NY) were pre-coated with goat anti-mouse IgG, and incubated with the capture mouse ALK antibody (Cat# 35-4300, Zymed, Seattle, WA) diluted 1:1000 in Superblock (Pierce, Rockford, IL). Following blocking, cell lysates were added to plates and incubated overnight at 4 $^\circ\text{C}$. Plates were incubated with the detecting antibody, anti-phospho-ALK (Y664) (Cell Signaling Technology), diluted at 1:2000, followed by incubation with goat anti-rabbit-IgG alkaline phosphatase to amplify the detection. Wells were exposed to the fluorogenic substrate 4-MeUP and the signal quantified using a CytoFluor[®] (series 4000) Fluorescence Multi-Well Plate Reader (Applied Biosystems, Foster City, CA).

5.5. 7-Iodo-3,4-dihydro-1H-pyrido[2,3-b]pyrazin-2-one (2)

2-Chloro-5-iodo-3-nitro-pyridine was dissolved in EtOH. Glycine ethyl ester HCl was added (5.0 equiv) followed by TEA

(5.0 equiv). The reaction mixture was heated to 80 °C for 4 h. The reaction mixture was concentrated to dryness and triturated with H₂O to obtain (5-iodo-3-nitro-pyridin-2-ylamino)-acetic acid ethyl ester as a white solid in 82–94% yield. Mp 200 °C (dec), LC–MS: $m/z = 352$ (M+H⁺), ¹H NMR (CDCl₃, 400 MHz) δ 1.30 (t, $J = 7.1$ Hz, 3H), 4.25 (q, $J = 7.1$ Hz, 2H), 4.33 (d, $J = 5.6$ Hz, 2H), 8.44 (br s, 1H), 8.52 (d, $J = 2.0$ Hz, 1H), 8.69 (d, $J = 2.0$ Hz, 1H). (5-Iodo-3-nitro-pyridin-2-ylamino)-acetic acid ethyl ester was dissolved in EtOH. SnCl₂·2H₂O was added and the reaction mixture was heated to 80 °C for 2 h. The resulting precipitate was filtered and washed with EtOH to afford **2** as a rust colored solid in 59–77% yield. Mp 81–82 °C, LC–MS: $m/z = 276$ (M+H⁺), ¹H NMR (DMSO-*d*₆, 400 MHz) δ 3.94 (s, 2H), 6.94 (br s, 1H), 7.12 (d, $J = 1.8$ Hz, 1H), 7.74 (s, $J = 1.8$ Hz, 1H), 10.40 (br s, 1H).

5.6. General procedure I. N-Benzyltion with NaH and benzyl bromides to form 3a–g

7-Iodo-3,4-dihydro-1H-pyrido[2,3-*b*]pyrazin-2-one (**2**) was suspended in anhydrous DMF and cooled to 0 °C. NaH (60% dispersion in mineral oil) (1 equiv) was added and a solution formed. The respective benzyl bromide (1 equiv) was added and the resulting reaction was stirred at rt for 1–4 h. The resulting product was purified by silica gel chromatography.

5.6.1. 1-Benzyl-7-iodo-3,4-dihydro-1H-pyrido[2,3-*b*]pyrazin-2-one (3a)

7-Iodo-3,4-dihydro-1H-pyrido[2,3-*b*]pyrazin-2-one **2** was treated with benzyl bromide following the conditions in general procedure I to obtain **3a** as a light yellow solid in 38% yield. Mp 225–226 °C, LC–MS: $m/z = 366$ (M+H⁺); calcd for C₁₄H₁₂N₃O: 366 (M+H⁺) ¹H NMR (DMSO-*d*₆, 400 MHz) δ 4.14 (s, 2H), 5.10 (s, 2H), 7.13 (s, 1H), 7.22–7.29 (m, 4H), 7.31–7.38 (m, 2H), 7.78 (s, 1H).

5.6.2. 1-(2,6-Dichloro-benzyl)-7-iodo-3,4-dihydro-1H-pyrido[2,3-*b*]pyrazin-2-one (3b)

7-Iodo-3,4-dihydro-1H-pyrido[2,3-*b*]pyrazin-2-one **2** was treated with 2,6-dichlorobenzyl bromide under the conditions of general procedure I to afford **3b** as an off-white solid. Mp >200 °C, LC–MS: $m/z = 434$ (M+H⁺); calcd for C₁₄H₁₀Cl₂IN₃O: 434 (M+H⁺), ¹H NMR (DMSO-*d*₆, 400 MHz) δ 3.30 (s, 2H), 5.29 (s, 2H), 7.31 (d, $J = 8.6$ Hz, 1H), 7.34 (d, $J = 7.6$ Hz, 1H), 7.45 (s, 1H), 7.47 (s, 1H), 7.76 (d, $J = 1.0$ Hz, 1H).

5.6.3. 1-(2,5-Difluoro-benzyl)-7-iodo-3,4-dihydro-1H-pyrido[2,3-*b*]pyrazin-2-one (3c)

7-Iodo-3,4-dihydro-1H-pyrido[2,3-*b*]pyrazin-2-one **2** was reacted with 2,5-difluorobenzyl bromide following the conditions in general procedure I to obtain **3c** as a tan solid in 70% yield. Mp >200 °C, LC–MS: $m/z = 402$ (M+H⁺), ¹H NMR (DMSO-*d*₆, 400 MHz) δ 4.13 (s, 2H), 5.09 (s, 2H), 7.01 (m, 1H), 7.15 (m, 2H), 7.28 (m, 1H), 7.80 (s, 1H).

5.6.4. 1-(2-Chloro-5-trifluoromethyl-benzyl)-7-iodo-3,4-dihydro-1H-pyrido[2,3-*b*]pyrazin-2-one (3d)

7-Iodo-3,4-dihydro-1H-pyrido[2,3-*b*]pyrazin-2-one **2** was reacted with 2-chloro-5-(trifluoromethyl) benzyl bromide following the conditions in general procedure I to afford **3d** as a white solid in 39% yield. Mp 252–253 °C, LC–MS: $m/z = 468$ (M+H⁺); calcd for C₁₅H₁₀ClF₃IN₃O: 468 (M+H⁺), ¹H NMR (DMSO-*d*₆, 400 MHz) δ 4.16 (d, $J = 1.2$ Hz, 2H), 5.16 (s, 2H), 7.20 (s, 1H), 7.26 (d, $J = 1.3$ Hz, 1H), 7.42 (s, 1H), 7.71 (dd, $J = 8.3$ Hz, 1.5 Hz, 1H), 7.77 (d, $J = 8.6$ Hz, 1H), 7.83 (d, $J = 1.5$ Hz, 1H).

5.6.5. 1-(5-Chloro-2-trifluoromethyl-benzyl)-7-iodo-3,4-dihydro-1H-pyrido[2,3-*b*]pyrazin-2-one (3e)

7-Iodo-3,4-dihydro-1H-pyrido[2,3-*b*]pyrazin-2-one **2** was reacted with 2-bromomethyl-4-chloro-1-trifluoromethyl-benzene following the conditions in general procedure I to obtain **3e** as a crude insoluble solid which was taken forward to 1-(5-chloro-2-trifluoromethyl-benzyl)-7-iodo-3,4-dihydro-1H-pyrido[2,3-*b*]pyrazin-2-one **4e** without further purification.

5.6.6. 1-(2,5-Dichloro-benzyl)-7-iodo-3,4-dihydro-1H-pyrido[2,3-*b*]pyrazin-2-one (3f)

7-Iodo-3,4-dihydro-1H-pyrido[2,3-*b*]pyrazin-2-one was reacted with 2,5-dichlorobenzyl bromide following the conditions in general procedure I to obtain **3f** as a brown solid in 69% yield. Mp >200 °C, LC–MS: $m/z = 434$ (M+H⁺); calcd for C₁₄H₁₀Cl₂IN₃O: 434 (M+H⁺), ¹H NMR (DMSO-*d*₆, 400 MHz) δ 4.18 (s, 2H), 5.07 (s, 2H), 7.14 (d, $J = 1.8$ Hz, 1H), 7.15 (d, $J = 2.3$ Hz, 1H), 7.40 (dd, $J = 8.6$, 2.5 Hz, 1H), 7.56 (d, $J = 8.6$ Hz, 1H), 7.85 (d, $J = 1.8$ Hz, 1H).

5.6.7. 1-(2-Chloro-3,6-difluoro-benzyl)-7-iodo-3,4-dihydro-1H-pyrido[2,3-*b*]pyrazin-2-one (3g)

7-Iodo-3,4-dihydro-1H-pyrido[2,3-*b*]pyrazin-2-one was reacted with 2-chloro-3,6-difluorobenzyl bromide following the conditions in general procedure I to afford **3g** as an off-white solid in 63% yield. Mp 237 °C, LC–MS: $m/z = 436$ (M+H⁺); calcd for C₁₄H₉ClF₂IN₃O: 436 (M+H⁺), ¹H NMR (DMSO-*d*₆, 400 MHz) δ 4.01 (s, 2H), 5.24 (s, 2H), 7.05 (d, $J = 1.5$ Hz, 1H), 7.23–7.32 (m, 1H), 7.41–7.48 (m, 1H), 7.79 (d, $J = 1.5$ Hz, 1H).

5.7. General procedure II. Amide reduction with DIBAL to form 4a–g

Compound **3** was suspended in anhydrous CH₂Cl₂ and cooled to 0 °C. DIBAL (8.0 equiv) was added and the resulting solution was allowed to warm to rt over 16 h. The reaction mixture was quenched with methanol and a saturated solution of potassium sodium tartrate was added. The mixture was stirred at rt until the layers separated (2 h), the layers were separated, and the organic layer was dried over MgSO₄, filtered, and concentrated. The product was purified via silica gel chromatography.

5.7.1. 1-Benzyl-7-iodo-1,2,3,4-tetrahydro-pyrido[2,3-*b*]pyrazine (4a)

1-Benzyl-7-iodo-3,4-dihydro-1H-pyrido[2,3-*b*]pyrazin-2-one (**3a**) was reduced via general procedure II to obtain **4a** as a light brown solid in 25% yield. Mp 147–148 °C, LC–MS: $m/z = 352$ (M+H⁺); calcd for C₁₄H₁₄IN₃: 351 (M+H⁺), ¹H NMR (CDCl₃, 400 MHz) δ 3.09–3.32 (m, 2H), 3.51–3.54 (m, 2H), 4.36 (s, 2H), 6.84 (s, 1H), 7.23–7.30 (m, 1H), 7.31–7.39 (m, 4H), 7.58 (d, $J = 1.5$ Hz, 1H).

5.7.2. 1-(2,6-Dichloro-benzyl)-7-iodo-1,2,3,4-tetrahydro-pyrido[2,3-*b*]pyrazine (4b)

1-(2,6-Dichloro-benzyl)-7-iodo-3,4-dihydro-1H-pyrido[2,3-*b*]pyrazin-2-one (**3b**) was reduced with general procedure II to afford **4b** as a light yellow solid. Mp >200 °C, LC–MS: $m/z = 420$ (M+H⁺); calcd for C₁₄H₁₂Cl₂IN₃: 420 (M+H⁺), ¹H NMR (CDCl₃, 400 MHz) δ 3.03 (t, $J = 4.8$ Hz, 2H), 3.42 (m, 2H), 4.48 (s, 2H), 4.81 (s, 1H), 7.09 (s, 1H), 7.24 (m, 1H), 7.36 (d, $J = 8.2$ Hz, 2H), 7.63 (d, $J = 1.6$ Hz, 1H).

5.7.3. 1-(2,5-Difluoro-benzyl)-7-iodo-1,2,3,4-tetrahydro-pyrido[2,3-*b*]pyrazine (4c)

1-(2,5-Difluoro-benzyl)-7-iodo-3,4-dihydro-1H-pyrido[2,3-*b*]pyrazin-2-one (**3c**) was reduced via general procedure II to afford **4c** as a white solid in 42% yield. Mp 175–176 °C, LC–MS: $m/z = 388$ (M+H⁺); calcd for C₁₄H₁₂F₂IN₃: 388 (M+H⁺), ¹H NMR (DMSO-*d*₆, 400 MHz) δ 3.26–3.30 (m, 2H), 3.36–3.42 (m, 2H), 4.44 (s, 2H),

6.63 (br s, 1H), 6.77 (s, 1H), 7.05–7.10 (m, 1H), 7.15–7.19 (m, 1H), 7.20–7.27 (m, 1H), 7.41 (s, 1H).

5.7.4. 1-(2-Chloro-5-trifluoromethyl-benzyl)-7-iodo-1,2,3,4-tetrahydro-pyrido[2,3-*b*]pyrazine (4d)

1-(2-Chloro-5-trifluoromethyl-benzyl)-7-iodo-3,4-dihydro-1H-pyrido[2,3-*b*]pyrazin-2-one (3d) was reduced with general procedure VI to obtain 4d as a yellow solid in 28% yield. Mp 120–125 °C, LC-MS: $m/z = 454$ (M+H⁺); calcd for C₁₅H₁₂ClF₃IN₃: 454 (M+H⁺), ¹H NMR (CDCl₃, 400 MHz) δ 3.38 (t, $J = 5.0$ Hz, 2H), 3.55–3.61 (m, 2H), 4.45 (s, 2H), 5.11 (s, 1H), 6.66 (s, 1H), 7.47 (s, 1H), 7.53 (dd, $J = 8.3$ Hz, 2H), 7.62 (d, $J = 1.8$ Hz, 1H).

5.7.5. 1-(5-Chloro-2-trifluoromethyl-benzyl)-7-iodo-1,2,3,4-tetrahydro-pyrido[2,3-*b*]pyrazine (4e)

1-(2-Chloro-5-trifluoromethyl-benzyl)-7-iodo-3,4-dihydro-1H-pyrido[2,3-*b*]pyrazin-2-one (3e) was reduced through general procedure II to afford 4e as an orange solid in 17% yield. Mp 189–191 °C, LC-MS: $m/z = 454$ (M+H⁺); calcd for C₁₅H₁₂ClF₃IN₃: 454 (M+H⁺), ¹H NMR (DMSO-*d*₆, 400 MHz) δ 3.28–3.34 (m, 2H), 3.41–3.46 (m, 2H), 4.53 (s, 2H), 6.52 (s, 1H), 6.75 (s, 1H), 7.44 (s, 2H), 7.59 (d, $J = 8.4$ Hz, 1H), 7.82 (d, $J = 8.6$ Hz, 1H).

5.7.6. 1-(2,5-Dichloro-benzyl)-7-iodo-1,2,3,4-tetrahydro-pyrido[2,3-*b*]pyrazine (4f)

1-(2,5-Dichloro-benzyl)-7-iodo-3,4-dihydro-1H-pyrido[2,3-*b*]pyrazin-2-one (3f) was reduced with general procedure II to obtain 4f as a brown solid in 85% yield. Mp 169–170 °C, LC-MS: $m/z = 421$ (M+H⁺); calcd for C₁₄H₁₂Cl₂IN₃: 421 (M+H⁺), ¹H NMR (CDCl₃, 400 MHz) δ 3.40 (m, 3H), 3.59 (m, 2H), 4.39 (s, 2H), 4.85 (br s, 1H), 6.64 (s, 1H), 7.18 (d, $J = 2.8$ Hz, 1H), 7.22 (dd, $J = 8.6, 2.8$ Hz, 1H), 7.35 (d, $J = 8.6$ Hz, 1H), 7.63 (d, $J = 1.5$ Hz, 1H).

5.7.7. 1-(2-Chloro-3,6-difluoro-benzyl)-7-iodo-1,2,3,4-tetrahydro-pyrido[2,3-*b*]pyrazine (4g)

1-(2-Chloro-3,6-difluoro-benzyl)-7-iodo-3,4-dihydro-1H-pyrido[2,3-*b*]pyrazin-2-one (3g) was reduced by general procedure II to afford 4g as an off-white solid in 42% yield. Mp 156–157 °C, LC-MS: $m/z = 422$ (M+H⁺); calcd for C₁₄H₁₁ClF₂IN₃: 422 (M+H⁺), ¹H NMR (CDCl₃, 400 MHz) δ 3.12–3.20 (m, 2H), 3.42–3.50 (m, 2H), 4.41 (s, 2H), 4.89 (br s, 1H), 6.98–7.05 (m, 1H), 7.08 (s, 1H), 7.10–7.18 (m, 1H), 7.62 (d, $J = 1.5$ Hz, 1H).

5.8. General procedure III. Suzuki coupling

General procedure IIIA: The starting iodo reactant was combined with an aryl boronate (1.2–2.0 equiv), Pd(PPh₃)₄ (0.02–0.05 equiv), and 2 M Na₂CO₃ (2.5 equiv) in a 6/1 mixture of toluene/EtOH. The resulting reaction mixture was heated to 80 °C for 1–16 h. The reaction mixture was then diluted with CH₂Cl₂, dried over MgSO₄, filtered, concentrated, and purified via silica gel chromatography.

General procedure IIIB: The starting iodo reactant, an aryl boronate, (1.5–2.0 equiv), and PdCl₂(PPh₃)₂ (0.1 equiv) were all dissolved in 6 mL THF. Potassium carbonate powder (5.0 equiv) was dissolved in 6 mL of water in a separate flask. The potassium carbonate solution was added to the boronate solution, the mixture was purged with nitrogen, and it was stirred at 70 °C for 1 h. The reaction mixture was concentrated, and methylene chloride and water were added. The aqueous layer was removed, and the organic layer was washed with saturated sodium bicarbonate solution, followed by brine. It was dried with magnesium sulfate, filtered, and then purified by silica gel column chromatography.

5.9. General procedure IV. Amide coupling

The Aryl carboxylic acid was combined in anhydrous DMF with *N*-(3-dimethylaminopropyl)-*N'*-ethylcarbodiimide hydrochloride

(2.0 equiv), 1-hydroxybenzotriazole (1.7 equiv), and triethylamine (1.4 equiv). After stirring at rt for 30 min, the respective amine was added. The reaction mixture was stirred for 3–16 h. The resulting reaction mixture was concentrated, diluted with CH₂Cl₂, washed with H₂O, dried over MgSO₄, and purified via silica gel chromatography or RP preparative HPLC.

5.9.1. [4-(1-Benzyl-1,2,3,4-tetrahydro-pyrido[2,3-*b*]pyrazin-7-yl)-phenyl]-((*S*)-2-pyrrolidinylmethyl-pyrrolidin-1-yl)-methanone—TFA salt (5a)

1-Benzyl-7-iodo-1,2,3,4-tetrahydro-pyrido[2,3-*b*]pyrazine (4a) was reacted with 4-ethoxycarbonyl phenyl boronic acid following general procedure IIIA to recover 4-(1-benzyl-1,2,3,4-tetrahydro-pyrido[2,3-*b*]pyrazin-7-yl)-benzoic acid ethyl ester as a pale yellow solid in 42% yield. Mp 178–179 °C, LC-MS: $m/z = 374$ (M+H⁺); calcd for C₂₃H₂₃ClN₃O₂: 374 (M+H⁺), ¹H NMR (CDCl₃, 400 MHz) δ 1.38 (t, $J = 7.1$ Hz, 3H), 3.40 (t, $J = 5.1$ Hz, 2H), 3.60–3.63 (m, 2H), 4.35 (q, $J = 7.1$ Hz, 2H), 4.48 (s, 2H), 6.85 (s, 1H), 7.27–7.49 (m, 5H), 7.43 (d, $J = 8.3$ Hz, 2H), 7.73 (d, $J = 2.0$ Hz, 2H), 8.00 (d, $J = 8.3$ Hz, 2H). 4-(1-Benzyl-1,2,3,4-tetrahydro-pyrido[2,3-*b*]pyrazin-7-yl)-benzoic acid ethyl ester was heated to 70 °C in a 1/1 mixture of THF and H₂O with 5 equiv LiOH·H₂O for 2–16 h. The resulting solution was concentrated and neutralized with 1 N HCl. The resulting precipitate was filtered to obtain 4-(1-benzyl-1,2,3,4-tetrahydro-pyrido[2,3-*b*]pyrazin-7-yl)-benzoic acid as a pale yellow solid in 90% yield. Mp >300 °C, LC-MS: $m/z = 346$ (M+H⁺); calcd for C₂₁H₁₉N₃O₂: 346 (M+H⁺), ¹H NMR (DMSO-*d*₆, 400 MHz) δ 3.35–3.38 (m, 2H), 3.52–3.54 (m, 2H), 4.62 (s, 2H), 7.08 (s, 1H), 7.25–7.27 (m, 1H), 7.29–7.32 (m, 4H), 7.62 (d, $J = 8.4$ Hz, 2H), 7.69 (d, $J = 1.8$ Hz, 1H), 7.92 (d, $J = 8.4$ Hz, 2H), 12.86 (br s, 1H). 4-(1-Benzyl-1,2,3,4-tetrahydro-pyrido[2,3-*b*]pyrazin-7-yl)-benzoic acid was coupled with (*S*)-(+)-1-(2-pyrrolidinylmethyl)pyrrolidine via general procedure IV. The reaction mixture was purified via RP preparative HPLC to obtain 5a as a yellow foam in 43% yield. LC-MS: $m/z = 482$ (M+H⁺); calcd for C₃₀H₃₅N₅O: 482 (M+H⁺), ¹H NMR (CDCl₃, 400 MHz) δ 1.82–1.84 (m, 1H), 1.92–2.05 (m, 2H), 2.06–2.20 (m, 4H), 2.92–3.08 (m, 1H), 3.18–3.25 (m, 1H), 3.25–3.35 (m, 1H), 3.39–3.48 (m, 2H), 3.50–3.52 (m, 1H), 3.55–3.63 (m, 1H), 3.65–3.71 (m, 1H), 3.72–3.77 (m, 2H), 3.82–3.94 (m, 1H), 4.01–4.11 (m, 1H), 4.48–4.59 (m, 3H), 6.92 (s, 1H), 7.26–7.42 (m, 8H), 7.56 (d, $J = 8.1$ Hz, 2H), 11.06 (br s, 1H).

5.9.2. {4-[1-(2,6-Dichloro-benzyl)-1,2,3,4-tetrahydro-pyrido[2,3-*b*]pyrazin-7-yl]-phenyl}-(2-pyrrolidin-1-ylmethyl-pyrrolidin-1-yl)-methanone (5b)

1-(2,6-Dichloro-benzyl)-7-iodo-1,2,3,4-tetrahydro-pyrido[2,3-*b*]pyrazine (4b) was reacted with (*S*)-2-pyrrolidin-1-ylmethyl-pyrrolidine-1-carboxylic acid [4-(4,4,5,5-tetramethyl-[1,3,2]dioxaborolan-2-yl)-phenyl]-amide [obtained through amide coupling of (*S*)-2-pyrrolidin-1-ylmethyl-pyrrolidine 4-(4,4,5,5-Tetramethyl-[1,3,2]dioxaborolan-2-yl)-benzoic acid using standard amide coupling conditions (EDCI, HOBT, DMF, DIEA, rt, 2 h)] following general procedure IIIB to obtain 5b as a yellow solid in 22% yield. LC-MS: $m/z = 550$ (M+H⁺); calcd for C₃₀H₃₃Cl₂N₅O: 550 (M+H⁺), ¹H NMR (CDCl₃, 400 MHz) δ 1.83 (m, 7H), 2.26 (m, 2H), 3.01 (m, 5H), 3.57 (m, 4H), 4.46 (br s, 1H), 4.61 (s, 2H), 5.17 (br s, 1H), 7.11 (d, $J = 1.5$ Hz, 1H), 7.25 (m, 1H), 7.37 (d, $J = 8.1$ Hz, 2H), 7.56 (m, 4H), 7.74 (s, 1H).

5.9.3. {4-[1-(2,5-Difluoro-benzyl)-1,2,3,4-tetrahydro-pyrido[2,3-*b*]pyrazin-7-yl]-phenyl}-((*S*)-2-pyrrolidin-1-ylmethyl-pyrrolidin-1-yl)-methanone (5c)

1-(2,5-Difluoro-benzyl)-7-iodo-1,2,3,4-tetrahydro-pyrido[2,3-*b*]pyrazine (4c) (500 mg) was reacted with 4-ethoxycarbonyl phenyl boronic acid following general procedure IIIA to obtain 4-[1-(2,5-difluoro-benzyl)-1,2,3,4-tetrahydro-pyrido[2,3-*b*]pyrazin-7-yl]-benzoic acid ethyl ester as an off-white solid in 63% yield.

Mp 173–174 °C, LC-MS: $m/z = 410$ ($M+H^+$); calcd for $C_{23}H_{21}F_2N_3O_2$: 410 ($M+H^+$), 1H NMR ($CDCl_3$, 400 MHz) δ 1.39 (t, $J = 7.1$ Hz, 3H), 3.45 (t, $J = 5.0$ Hz, 2H), 3.61–3.66 (m, 2H), 4.37 (q, $J = 7.1$ Hz, 2H), 4.49 (s, 2H), 5.32 (br s, 1H), 6.78 (d, $J = 1.5$ Hz, 1H), 6.89–6.96 (m, 1H), 6.99–7.08 (m, 2H), 7.45 (d, $J = 8.4$ Hz, 2H), 7.76 (d, $J = 1.8$ Hz, 2H), 8.02 (d, $J = 8.6$ Hz, 2H). 4-[1-(2,5-Difluoro-benzyl)-1,2,3,4-tetrahydro-pyrido[2,3-*b*]pyrazin-7-yl]-benzoic acid ethyl ester was heated to 70 °C in a 1/1 mixture of THF and H_2O with 5 equiv LiOH· H_2O for 2–16 h. The resulting solution was concentrated and neutralized with 1 N HCl. The resulting precipitate was filtered to obtain 4-[1-(2,5-difluoro-benzyl)-1,2,3,4-tetrahydro-pyrido[2,3-*b*]pyrazin-7-yl]-benzoic acid as a beige solid in 91% yield. Mp >300 °C, LC-MS: $m/z = 382$ ($M+H^+$); calcd for $C_{21}H_{17}F_2N_3O_2$: 382 ($M+H^+$), 1H NMR ($DMSO-d_6$, 400 MHz) δ 3.28–3.33 (m, 2H), 3.40–3.49 (m, 2H), 4.58 (s, 2H), 6.58 (s, 1H), 6.77 (s, 1H), 7.10–7.20 (m, 2H), 7.26–7.34 (m, 1H), 7.59 (d, $J = 8.3$ Hz, 2H), 7.73 (s, 1H), 7.89 (d, $J = 8.3$ Hz, 2H), 12.92 (br s, 1H). 4-[1-(2,5-Difluoro-benzyl)-1,2,3,4-tetrahydro-pyrido[2,3-*b*]pyrazin-7-yl]-benzoic acid was reacted with (S)-(+)-1-(2-pyrrolidinylmethyl)pyrrolidine following general procedure IV to obtain **5c** as a pale yellow solid in 53% yield. Mp 143–144 °C, LC-MS: $m/z = 518$ ($M+H^+$); calcd for $C_{30}H_{33}F_2N_5O$: 518 ($M+H^+$), 1H NMR ($CDCl_3$, 400 MHz) δ 1.48–1.58 (m, 1H), 1.87–2.15 (m, 4H), 2.17–2.22 (m, 3H), 2.55–2.64 (m, 4H), 2.83–2.89 (m, 1H), 3.12–3.23 (m, 1H), 3.42–3.50 (m, 2H), 3.60–3.64 (m, 2H), 4.40–4.49 (m, 3H), 5.07 (br s, 1H), 6.76 (s, 1H), 6.86–7.09 (m, 3H), 7.41 (d, $J = 8.1$ Hz, 2H), 7.45–7.52 (m, 2H), 7.73 (s, 1H).

5.9.4. 1-(2,5-Difluoro-benzyl)-7-[6-(4-methyl-piperazin-1-yl)-pyridin-3-yl]-1,2,3,4-tetrahydro-pyrido[2,3-*b*]pyrazine (**5d**)

1-(2,5-Difluoro-benzyl)-7-iodo-1,2,3,4-tetrahydro-pyrido[2,3-*b*]pyrazine (**4c**) was reacted with 1-methyl-4-[5-(4,4,5,5-tetramethyl-[1,3,2]dioxaborolan-2-yl)-pyridin-2-yl]-piperazine following general procedure IIIA to afford **5d** as a beige solid in 53% yield. Mp 192–193 °C, LC-MS: $m/z = 437$ ($M+H^+$); calcd for $C_{24}H_{26}F_2N_6$: 437 ($M+H^+$), 1H NMR ($CDCl_3$, 400 MHz) δ 2.34 (s, 3H), 2.52–2.58 (m, 4H), 3.43–3.50 (m, 2H), 3.52–3.59 (m, 4H), 3.60–3.65 (m, 2H), 4.47 (s, 2H), 4.90 (s, 1H), 6.62 (m, 2H), 6.91–7.09 (m, 3H), 7.52 (dd, $J = 8.8$ Hz, 2.5 Hz, 1H), 7.62 (d, $J = 1.8$ Hz, 1H), 8.2 (d, $J = 2.5$ Hz, 1H).

5.9.5. 1-(5-Chloro-2-trifluoromethyl-benzyl)-7-[6-(4-methyl-piperazin-1-yl)-pyridin-3-yl]-1,2,3,4-tetrahydro-pyrido[2,3-*b*]pyrazine (**5e**)

1-(5-Chloro-2-trifluoromethyl-benzyl)-7-iodo-1,2,3,4-tetrahydro-pyrido[2,3-*b*]pyrazine (**4e**) was reacted with 1-methyl-4-[5-(4,4,5,5-tetramethyl-[1,3,2]dioxaborolan-2-yl)-pyridin-2-yl]-piperazine following general procedure IIA to obtain **5e** as a pale orange solid in 28% yield. Mp 226–227 °C, LC-MS: $m/z = 504$ ($M+H^+$); calcd for $C_{25}H_{26}ClF_3N_6$: 504 ($M+H^+$), 1H NMR ($CDCl_3$, 400 MHz) δ 2.34 (s, 3H), 2.51 (t, $J = 5.0$ Hz, 4H), 3.47–3.56 (m, 6H), 3.62–3.69 (m, 2H), 4.61 (s, 2H), 4.92 (br s, 1H), 6.49 (d, $J = 1.0$ Hz, 1H), 6.64 (d, $J = 8.8$ Hz, 1H), 7.34 (d, $J = 8.3$ Hz, 1H), 7.52–7.58 (m, 2H), 7.61–7.65 (m, 2H), 8.18 (d, $J = 2.3$ Hz, 1H).

5.9.6. 1-(2-Chloro-5-trifluoromethyl-benzyl)-7-[6-(4-methyl-piperazin-1-yl)-pyridin-3-yl]-1,2,3,4-tetrahydro-pyrido[2,3-*b*]pyrazine (**5f**)

1-(2-Chloro-5-trifluoromethyl-benzyl)-7-iodo-1,2,3,4-tetrahydro-pyrido[2,3-*b*]pyrazine (**4d**) was reacted with 1-methyl-4-[5-(4,4,5,5-tetramethyl-[1,3,2]dioxaborolan-2-yl)-pyridin-2-yl]-piperazine following general procedure IIA to obtain **5f** as a yellow film in 13% yield. LC-MS: $m/z = 503$ ($M+H^+$); calcd for $C_{25}H_{26}ClF_3N_6$: 503 ($M+H^+$), 1H NMR ($CDCl_3$, 400 MHz) δ 2.34 (s, 3H), 2.51 (t, $J = 5.3$ Hz, 4H), 3.28 (t, $J = 5.3$ Hz, 2H), 3.54 (t, $J = 5.0$ Hz, 4H), 3.66–3.72 (m, 2H), 4.53 (s, 2H), 4.89 (br s, 1H), 6.53 (s, 1H), 6.64 (d, $J = 8.8$ Hz,

1H), 7.46–7.54 (m, 4H), 7.63 (d, $J = 1.8$ Hz, 1H), 8.18 (d, $J = 2.3$ Hz, 1H).

5.9.7. 1-(2,5-Dichloro-benzyl)-7-[6-(4-methyl-piperazin-1-yl)-pyridin-3-yl]-1,2,3,4-tetrahydro-pyrido[2,3-*b*]pyrazine (**5g**)

1-(2,5-Dichloro-benzyl)-7-iodo-1,2,3,4-tetrahydro-pyrido[2,3-*b*]pyrazine (**4f**) was coupled to 1-methyl-4-[5-(4,4,5,5-tetramethyl-[1,3,2]dioxaborolan-2-yl)-pyridin-2-yl]-piperazine following general procedure IIB to afford **5g** as a brown solid in 50% yield. LC-MS: $m/z = 469$ ($M+H^+$); calcd for $C_{24}H_{26}Cl_2N_6$: 469 ($M+H^+$), 1H NMR ($CDCl_3$, 400 MHz) δ 2.33 (s, 3H), 2.51 (t, $J = 5.1$ Hz, 4H), 3.48 (m, 2H), 3.55 (t, $J = 5.1$ Hz, 4H), 3.64 (t, $J = 4.7$ Hz, 2H), 4.46 (s, 2H), 5.20 (br s, 1H), 6.52 (d, $J = 1.5$ Hz, 1H), 6.65 (d, $J = 8.8$ Hz, 1H), 7.19 (dd, $J = 8.5$, 2.4 Hz, 1H), 7.26 (d, $J = 2.3$ Hz, 1H), 7.33 (d, $J = 8.3$ Hz, 1H), 7.52 (dd, $J = 8.6$, 2.5 Hz, 1H), 7.62 (d, $J = 1.5$ Hz, 1H), 8.20 (d, $J = 2.5$ Hz, 1H).

5.9.8. 1-(2-Chloro-3,6-difluoro-benzyl)-7-[6-(4-methyl-piperazin-1-yl)-pyridin-3-yl]-1,2,3,4-tetrahydro-pyrido[2,3-*b*]pyrazine (**5h**)

1-(2-Chloro-3,6-difluoro-benzyl)-7-iodo-1,2,3,4-tetrahydro-pyrido[2,3-*b*]pyrazine (**4g**) was coupled to 1-methyl-4-[5-(4,4,5,5-tetramethyl-[1,3,2]dioxaborolan-2-yl)-pyridin-2-yl]-piperazine through general procedure IIB to afford **5h** as a light brown solid in 16% yield. Mp = 219–220 °C, LC-MS: $m/z = 471$ ($M+H^+$); calcd for $C_{24}H_{25}ClF_2N_6$: 471 ($M+H^+$), 1H NMR ($CDCl_3$, 400 MHz) δ 2.36 (s, 3H), 2.54 (t, $J = 5.1$ Hz, 4H), 3.27 (t, $J = 4.8$ Hz, 2H), 3.51 (t, $J = 4.7$ Hz, 2H), 3.59 (t, $J = 5.1$ Hz, 4H), 4.50 (d, $J = 1.0$ Hz, 2H), 5.01 (br s, 1H), 6.70 (d, $J = 8.8$ Hz, 1H), 7.03 (m, 2H), 7.11 (m, 1H), 7.61 (dd, $J = 8.8$, 2.5 Hz, 1H), 7.64 (d, $J = 1.8$ Hz, 1H), 8.35 (d, $J = 2.3$ Hz, 1H).

5.9.9. 4-[1-[5-Chloro-2-(trifluoromethyl)benzyl]-1,2,3,4-tetrahydropyrido[2,3-*b*]pyrazin-7-yl]benzoic acid ethyl ester (**5i**)

1-[5-Chloro-2-(trifluoromethyl)benzyl]-7-iodo-1,2,3,4-tetrahydropyrido[2,3-*b*]pyrazine (7.0 g) was reacted with 4-ethoxycarbonyl phenyl boronic acid as in general procedure IIIA. **5i** was obtained as a yellow solid in 71% yield. Mp 154–155 °C, LC-MS: $m/z = 476$ ($M+H^+$); calcd for $C_{24}H_{21}ClF_3N_3O_2$: 476 ($M+H^+$), 1H NMR ($CDCl_3$, 400 MHz) δ 1.40 (t, 3H), 3.49 (m, 2H), 3.71 (m, 2H), 4.35 (q, 2H), 4.61 (s, 2H), 5.72 (br s, 1H), 6.62 (s, 1H), 7.44 (m, 3H), 7.50 (s, 1H), 7.63 (d, 1H), 7.72 (s, 1H), 8.07 (d, 2H).

5.9.10. 4-[1-[5-Chloro-2-(trifluoromethyl)benzyl]-1,2,3,4-tetrahydropyrido[2,3-*b*]pyrazin-7-yl]benzoic acid (**5j**)

4-[1-[5-Chloro-2-(trifluoromethyl)benzyl]-1,2,3,4-tetrahydropyrido[2,3-*b*]pyrazin-7-yl]benzoic acid ethyl ester (**5i**) (5.1 g) was heated to 70 °C in a 1/1 mixture of THF and H_2O with 5 equiv LiOH· H_2O for 2–16 h. The resulting solution was concentrated and neutralized with 1 N HCl. The resulting precipitate was filtered to obtain **5j** as a light orange solid in 88% yield. LC-MS: $m/z = 448$ ($M+H^+$); calcd for $C_{22}H_{17}ClF_3N_3O_2$: 448 ($M+H^+$), 1H NMR ($DMSO-d_6$, 400 MHz) δ 3.41 (m, 2H), 3.60 (m, 2H), 4.80 (s, 2H), 7.07 (s, 1H), 7.63 (m, 3H), 7.74 (s, 1H), 7.82 (d, 1H), 7.95 (m, 2H), 8.81 (s, 1H), 13.01 (br s, 1H).

5.9.11. {1-[5-Chloro-2-(trifluoromethyl)benzyl]-1,2,3,4-tetrahydro-pyrido[2,3-*b*]pyrazin-7-yl]piperidin-1-yl-methanone (**5k**)

4-[1-[5-Chloro-2-(trifluoromethyl)benzyl]-1,2,3,4-tetrahydropyrido[2,3-*b*]pyrazin-7-yl]benzoic acid (**5j**) (89 mg) was reacted with piperidine as in general procedure IV to give **5k** as an orange solid in 64% yield. Mp 216–217 °C, LC-MS: $m/z = 515$ ($M+H^+$); calcd for $C_{27}H_{26}ClF_3N_4O$: 515 ($M+H^+$), 1H NMR ($CDCl_3$, 400 MHz) δ 1.61 (m, 6H), 2.88 (s, 1H), 2.95 (s, 1H), 3.38 (s, 2H), 3.49 (m, 2H), 3.69

(m, 2H), 4.62 (s, 2H), 5.26 (s, 1H), 6.60 (s, 1H), 7.37 (m, 5H), 7.51 (s, 1H), 7.64 (d, $J = 8.3$ Hz, 1H), 7.75 (d, $J = 1.5$ Hz, 1H).

5.9.12. {1-[(5-Chloro-2-trifluoromethyl)benzyl]-1,2,3,4-tetrahydro-pyrido[2,3-*b*]pyrazin-7-yl)-(4-methoxy-piperidin-1-yl)-methanone (5l)}

4-[1-[5-Chloro-2-(trifluoromethyl)benzyl]-1,2,3,4-tetrahydro-pyrido[2,3-*b*]pyrazin-7-yl]benzoic acid (**5j**) (80 mg) was reacted with 4-methoxypiperidine HCl as in general procedure IV to give **5l** as an orange solid in 58% yield. LC-MS: $m/z = 545$ ($M+H^+$); calcd for $C_{28}H_{28}ClF_3N_4O_2$: 545 ($M+H^+$), 1H NMR ($CDCl_3$, 400 MHz) δ 1.73 (m, 4H), 2.88 (s, 1H), 2.95 (s, 1H), 3.36 (s, 3H), 3.47 (m, 4H), 3.68 (m, 3H), 4.62 (s, 2H), 5.35 (br s, 1H), 6.59 (d, $J = 1.3$ Hz, 1H), 7.38 (m, 5H), 7.51 (s, 1H), 7.64 (d, $J = 8.3$ Hz, 1H), 7.75 (s, 1H).

5.9.13. {4-[1-(5-Chloro-2-trifluoromethyl-benzyl)-1,2,3,4-tetrahydro-pyrido[2,3-*b*]pyrazin-7-yl]-phenyl)-(4-pyrrolidin-1-yl)-piperidin-1-yl)-methanone (5m)}

1-(5-Chloro-2-trifluoromethyl-benzyl)-7-iodo-1,2,3,4-tetrahydro-pyrido[2,3-*b*]pyrazine (**4e**) was reacted with (4-pyrrolidin-1-yl)-piperidin-1-yl-[4-(4,4,5,5-tetramethyl [1,3,2]dioxaborolan-2-yl)-phenyl]-methanone following general procedure IIIA to obtain **5m** as an orange foam in 19% yield. LC-MS: $m/z = 585$ ($M+H^+$); calcd for $C_{31}H_{33}ClF_3N_5O$: 585 ($M+H^+$), 1H NMR ($CDCl_3$, 400 MHz) δ 1.43–1.62 (m, 3H), 1.65–1.99 (m, 3H), 2.21–2.30 (m, 2H), 2.52–2.61 (m, 6H), 2.87–3.08 (m, 3H), 3.47–3.51 (m, 2H), 3.65–3.71 (m, 2H), 4.62 (s, 2H), 5.02 (s, 1H), 6.59 (d, $J = 1.5$ Hz, 1H), 7.31–7.39 (m, 5H), 7.50 (s, 1H), 7.65 (d, $J = 8.4$ Hz, 1H), 7.74 (s, 1H).

5.9.14. 1-(5-Chloro-2-trifluoromethyl-benzyl)-7-(2-piperazin-1-yl-pyridin-4-yl)-1,2,3,4-tetrahydro-pyrido[2,3-*b*]pyrazine (5n)}

1-(5-Chloro-2-trifluoromethyl-benzyl)-7-iodo-1,2,3,4-tetrahydro-pyrido[2,3-*b*]pyrazine (**4e**) was reacted with 2-(piperazin-1-yl)pyridine-4-boronic acid pinacol ester following general procedure IIIB to obtain **5n** as an off-white solid. Mp 189–190 °C, LC-MS: $m/z = 489$; calcd for $C_{24}H_{24}ClF_3N_6$: 489 ($M+H^+$), 1H NMR ($CDCl_3$, 400 MHz) δ 2.98 (m, 4H), 3.49 (6H, m), 3.71 (m, 2H), 4.61 (s, 2H), 5.29 (s, 1H), 5.34 (br s, 1H), 6.55 (m, 2H), 6.64 (dd, $J = 5.2, 1.4$ Hz, 1H), 7.36 (d, $J = 8.1$ Hz, 1H), 7.52 (s, 1H), 7.64 (d, $J = 8.3$ Hz, 1H), 7.77 (d, $J = 2.0$ Hz, 1H), 8.12 (d, $J = 5.3$ Hz, 1H).

5.9.15. 1-[4-(4-[1-[5-Chloro-2-(trifluoromethyl)benzyl]-1,2,3,4-tetrahydro-pyrido[2,3-*b*]pyrazin-7-yl]pyridin-2-yl)piperazin-1-yl]ethanone (5o)}

To a solution of 1-[5-chloro-2-(trifluoromethyl)benzyl]-7-(2-piperazin-1-yl-pyridin-4-yl)-1,2,3,4-tetrahydro-pyrido[2,3-*b*]pyrazine (**5n**) (63 mg) in anhydrous DMF (1 mL) was added acetyl chloride (1.3 equiv) and triethylamine (1.1 equiv). The mixture was stirred at room temperature under nitrogen overnight and then concentrated. The residue was purified on normal phase silica gel chromatography to give **5o** as a yellow solid in 56% yield. Mp 241–242 °C, LC-MS: $m/z = 531$ (calcd for $C_{26}H_{26}ClF_3N_6O$: 531 ($M+H^+$), 1H NMR ($CDCl_3$, 400 MHz) δ 2.15 (s, 3H), 3.47 (m, 2H), 3.52 (m, 2H), 3.57 (m, 2H), 3.62 (m, 2H), 3.73 (m, 4H), 4.61 (s, 2H), 5.25 (br s, 1H), 6.55 (m, 2H), 6.69 (d, $J = 5.3$ Hz, 1H), 7.37 (d, $J = 8.3$ Hz, 1H), 7.52 (s, 1H), 7.65 (d, $J = 8.3$ Hz, 1H), 7.78 (br s, 1H), 8.12 (d, $J = 5.3$ Hz, 1H).

5.9.16. 1-(2,5-Difluoro-benzenesulfonyl)-7-[6-(4-methyl-piperazin-1-yl)-pyridin-3-yl]-1,2,3,4-tetrahydro-pyrido[2,3-*b*]pyrazine (9a)}

7-Iodo-3,4-dihydro-1*H*-pyrido[2,3-*b*]pyrazin-2-one was treated with general procedure V using 4 equiv DIBAL-H to obtain 7-iodo-1,2,3,4-tetrahydro-pyrido[2,3-*b*]pyrazine as a white solid in 31% yield. Mp 126–128 °C, LC-MS: $m/z = 262$ ($M+H^+$); calcd for $C_7H_8IN_3$: 262 ($M+H^+$), 1H NMR ($DMSO-d_6$, 400 MHz) δ 3.13–3.17

(m, 2H), 3.27–3.29 (m, 2H), 5.78 (s, 1H), 6.37 (s, 1H), 6.78 (d, $J = 2.0$ Hz, 1H), 7.33 (d, $J = 2.0$ Hz, 1H). 7-Iodo-1,2,3,4-tetrahydro-pyrido[2,3-*b*]pyrazine (**7**) was dissolved in anhydrous pyridine. 2,5-Difluorobenzene sulfonyl chloride (1.0 equiv) was added and the reaction mixture was stirred at rt for 16 h. The reaction mixture was concentrated and the resulting residue was purified by silica gel chromatography to afford 1-(2,5-difluoro-benzenesulfonyl)-7-iodo-1,2,3,4-tetrahydro-pyrido[2,3-*b*]pyrazine (**8**) as a pale yellow solid in 13% yield. Mp 187–188 °C, LC-MS: $m/z = 438$ ($M+H^+$); calcd for $C_{13}H_{10}F_2N_3O_2S$: 438 ($M+H^+$), 1H NMR ($CDCl_3$, 400 MHz) δ 3.29–3.33 (m, 2H), 3.83 (t, $J = 4.8$ Hz, 2H), 5.08 (br s, 1H), 7.11–7.19 (m, 1H), 7.26–7.33 (m, 1H), 7.58–7.63 (m, 1H), 7.96 (d, $J = 1.5$ Hz, 1H), 8.03 (d, $J = 1.8$ Hz, 1H). 1-(2,5-Difluoro-benzenesulfonyl)-7-iodo-1,2,3,4-tetrahydro-pyrido[2,3-*b*]pyrazine (**8**) was reacted with 1-methyl-4-[5-(4,4,5,5-tetramethyl-[1,3,2]dioxaborolan-2-yl)-pyridin-2-yl]-piperazine following general procedure IIIA to obtain **9a** as a yellow foam in 35% yield. LC-MS: $m/z = 487$ ($M+H^+$); calcd for $C_{23}H_{26}F_2N_6O_2S$: 487 ($M+H^+$), 1H NMR ($CDCl_3$, 400 MHz) δ 2.34 (s, 3H), 2.54 (t, $J = 5.3$ Hz, 4H), 3.35–3.38 (m, 2H), 3.60 (t, $J = 5.0$ Hz, 4H), 3.91 (t, $J = 4.8$ Hz, 2H), 5.05 (br s, 1H), 6.71 (d, $J = 8.8$ Hz, 1H), 7.11–7.17 (m, 1H), 7.24–7.29 (m, 1H), 7.58–7.63 (m, 2H), 7.90 (d, $J = 2.0$ Hz, 1H), 8.05 (d, $J = 2.3$ Hz, 1H), 8.34 (d, $J = 2.6$ Hz, 1H).

5.9.17. (2,5-Difluoro-phenyl)-{7-[4-((S)-2-pyrrolidin-1-ylmethyl-pyrrolidine-1-carbonyl)-phenyl]-3,4-dihydro-2*H*-pyrido[2,3-*b*]pyrazin-1-yl)-methanone (9b)}

7-Iodo-1,2,3,4-tetrahydro-pyrido[2,3-*b*]pyrazine was dissolved in anhydrous THF. Pyridine (1.0 equiv) was added, and the reaction was cooled to 0 °C. 2,5-Difluorophenyl acetyl chloride (1.0 equiv) was added, and a white precipitate formed. The reaction was stirred at 0 °C for 15 min, allowed to warm to rt, and stirred at rt for 16 h. The reaction was diluted with EtOAc, washed with $NaHCO_3$, dried over $MgSO_4$, filtered, concentrated, and purified by silica gel chromatography to afford (2,5-difluoro-phenyl)-(7-iodo-3,4-dihydro-2*H*-pyrido[2,3-*b*]pyrazin-1-yl)-methanone as an off-white solid in 14% yield. Mp 152–153 °C, LC-MS: $m/z = 416$ ($M+H^+$); calcd for $C_{15}H_{12}F_2IN_3O$: 416 ($M+H^+$), 1H NMR ($CDCl_3$, 400 MHz) δ 3.47–3.54 (m, 2H), 3.80–3.87 (m, 4H), 5.44 (br s, 1H), 6.90–7.04 (m, 3H), 8.03 (s, 1H). 2-(2,5-Difluoro-phenyl)-1-(7-iodo-3,4-dihydro-2*H*-pyrido[2,3-*b*]pyrazin-1-yl)-ethanone was reacted with 1-methyl-4-[5-(4,4,5,5-tetramethyl-[1,3,2]dioxaborolan-2-yl)-pyridin-2-yl]-piperazine following general procedure IIIA to afford 2-(2,5-difluoro-phenyl)-1-[7-[2-(4-methyl-piperazin-1-yl)-pyridin-4-yl]-3,4-dihydro-2*H*-pyrido[2,3-*b*]pyrazin-1-yl]-ethanone as a light yellow solid in 15% yield. Mp >300 °C, LC-MS: $m/z = 465.02$ ($M+H^+$); calcd for $C_{25}H_{26}F_2N_6O$: 465 ($M+H^+$), 1H NMR ($CDCl_3$, 400 MHz) δ 2.36 (s, 3H), 2.52–2.57 (m, 2H), 3.52–3.62 (m, 6H), 3.90–3.96 (m, 4H), 5.11 (br s, 1H), 6.70 (d, $J = 8.8$ Hz, 1H), 6.90–7.04 (m, 3H), 7.41–7.58 (m, 2H), 8.07 (s, 1H), 8.32 (s, 1H).

5.9.18. 7-Bromo-1,2,3,4-tetrahydro-[1,8]naphthyridin-4-ol (11)}

7-Bromo-2,3-dihydro-1*H*-[1,8]naphthyridin-4-one (**10**) was placed in methanol and sodium borohydride (1.84 equiv) was added portionwise over 5 min. The reaction was stirred at rt for 15 min and then quenched with acetic acid. The reaction mixture was concentrated under reduced pressure and the residue was taken up in toluene. Silica gel was added and the mixture was concentrated under reduced pressure. Purification by silica gel chromatography using dry loading and a gradient of 0–80% EtOAc/hex as the eluting solvent afforded **11** as a pale yellow solid in 78% yield. Mp 130–131 °C, LC-MS: $m/z = 231$ ($M+H^+$); calcd for $C_8H_9BrN_2O$: 230 ($M+H^+$), 1H NMR ($MeOH-d_4$, 400 MHz) δ 1.80–1.94 (m, 2H), 3.33–3.48 (m, 2H), 4.66 (t, $J = 4.4$ Hz, 1H), 6.66 (d, $J = 7.6$ Hz, 1H), 7.31 (d, $J = 7.6$ Hz, 1H).

5.9.19. 6-Bromo-1,2,3,4-tetrahydro-[1,8]naphthyridin-4-ol (12)

7-Bromo-1,2,3,4-tetrahydro-[1,8]naphthyridin-4-ol (**11**) was dissolved in anhydrous THF and cooled to -78°C . A solution of *n*-butyllithium in THF was added (5–7 equiv) and the reaction was warmed slowly to room temperature. After 2–5 h, methanol was added and the contents were concentrated to dryness. The residue was dissolved in DCM/AcOH (1:1) and NBS (1.2 equiv) was added. After 45 min, the mixture was concentrated to dryness onto silica gel, and purified by silica gel chromatography to afford **12** as yellow solids in 25–65% yield. Mp $125\text{--}128^{\circ}\text{C}$, LC–MS: $m/z = 229$ ($\text{M}+\text{H}^+$); calcd for $\text{C}_8\text{H}_9\text{Br}_2\text{N}_2\text{O}$: 230 ($\text{M}+\text{H}^+$), ^1H NMR (DMSO- d_6 , 400 MHz) δ 1.72 (m, 2H), 3.25 (m, 2H), 4.56 (m, 1H), 5.33 (d, $J = 5.0$ Hz, 1H), 6.8 (br s, 1H), 7.47 (d, $J = 2.5$ Hz, 1H), 7.87 (d, $J = 2.5$ Hz, 1H).

5.9.20. 6-[6-(4-Methyl-piperazin-1-yl)-pyridin-3-yl]-1,2,3,4-tetrahydro-[1,8]naphthyridin-4-ol (13)

6-Bromo-1,2,3,4-tetrahydro-[1,8]naphthyridin-4-ol (**12**) was reacted with 1-methyl-4-[5-(4,4,5,5-tetramethyl-[1,3,2] dioxaborolan-2-yl)-pyridin-2-yl]-piperazine following general procedure IIIA. The product was purified by silica gel chromatography using a gradient of 0–10% (5% NH_4OH in MeOH)/ CH_2Cl_2 as the eluting solvent to obtain **13** as brown solids in 22% yield. Mp $124\text{--}128^{\circ}\text{C}$, LC–MS: $m/z = 326$ ($\text{M}+\text{H}^+$); calcd for $\text{C}_{18}\text{H}_{23}\text{N}_5\text{O}$: 326 ($\text{M}+\text{H}^+$), ^1H NMR (CDCl_3 , 400 MHz) δ 2.00 (m, 1H), 2.08 (s, 1H), 2.62 (t, $J = 5.0$ Hz, 4H), 3.49 (m, 2H), 3.58 (m, 2H), 3.63 (t, $J = 5.0$ Hz, 4H), 4.85 (t, $J = 4.0$ Hz, 1H), 6.68 (s, 1H), 6.71 (s, 1H), 7.59 (dd, $J = 2.6$, 8.8 Hz, 1H), 7.66 (d, $J = 2.2$ Hz, 1H), 8.01 (d, $J = 2.3$ Hz, 1H), 8.32 (d, $J = 2.5$ Hz, 1H).

5.9.21. 4-(2-Chloro-3,6-difluoro-phenoxy)-6-[6-(4-methyl-piperazin-1-yl)-pyridin-3-yl]-1,2,3,4-tetrahydro-[1,8]naphthyridine (14)

6-[6-(4-Methyl-piperazin-1-yl)-pyridin-3-yl]-1,2,3,4-tetrahydro-[1,8]naphthyridin-4-ol (**13**) (1 equiv), 2-chloro-3,6-difluorophenol (1–3.0 equiv), and triphenylphosphine (1–3.0 equiv) were placed in anhydrous THF and DIAD (3.0 equiv) was added. The reaction mixture was stirred at rt for 15 min and then concentrated under reduced pressure. The resulting crude product was purified by silica gel chromatography using a gradient of 0–10% MeOH/ CH_2Cl_2 as the eluting solvent to obtain **14** as a yellow foam in 54% yield. LC–MS: $m/z = 472$ ($\text{M}+\text{H}^+$); calcd for $\text{C}_{24}\text{H}_{24}\text{ClF}_2\text{N}_5\text{O}$: 472 ($\text{M}+\text{H}^+$), ^1H NMR (DMSO- d_6 , 400 MHz) δ 1.89 (m, 1H), 2.21 (s, 3H), 2.24 (m, 1H), 2.39 (t, $J = 4.8$ Hz, 4H), 3.40 (m, 1H), 3.47 (t, $J = 4.8$ Hz, 4H), 3.63 (m, 1H), 6.82 (d, $J = 8.8$ Hz, 1H), 7.03 (d, $J = 2.3$ Hz, 1H), 7.17 (d, $J = 2.3$ Hz, 1H), 7.25 (m, 1H), 7.39 (m, 1H), 7.52 (dd, $J = 2.5$, 8.8 Hz, 1H), 8.08 (d, $J = 2.5$ Hz, 1H), 8.19 (d, $J = 2.5$ Hz, 1H).

5.9.22. 7-Bromo-4-[1-iodo-methylidene]-1,2,3,4-tetrahydro-[1,8] naphthyridine (15)

7-Bromo-2,3-dihydro-1H-[1,8]naphthyridin-4-one (**10**)³² was suspended in anhydrous THF and a solution of CrCl_2 (8.35 equiv) and CHI_3 (2.13 equiv) in anhydrous THF was added. The reaction was stirred at rt for 16 h and was then diluted with methylene chloride and washed with saturated NaHCO_3 . The aqueous phase was extracted twice with methylene chloride and the combined organic layers were washed with brine and then dried over Na_2SO_4 . The solution was filtered and concentrated under reduced pressure. Purification by silica gel chromatography using a gradient of 0–30% EtOAc/hex as the eluting solvent to obtain **15** as a yellow solid in 27% yield. Alkene geometry determined by NOE. LC–MS: $m/z = 352$ ($\text{M}+\text{H}^+$); calcd for $\text{C}_9\text{H}_8\text{BrIN}_2$: 352 ($\text{M}+\text{H}^+$), ^1H NMR (CDCl_3 , 400 MHz) δ 2.69 (t, $J = 6.0$ Hz, 2H), 3.43–3.51 (m, 2H), 5.25 (br s, 1H), 6.23 (s, 1H), 6.74 (d, $J = 8.0$ Hz, 1H), 8.19 (d, $J = 8.0$ Hz, 1H).

5.9.23. 7-Bromo-4-[1-(2,5-difluoro-phenyl)-methylidene]-1,2,3,4-tetrahydro [1,8]naphthyridine (16)

7-Bromo-4-[1-iodo-methylidene]-1,2,3,4-tetrahydro-[1,8]naphthyridine, 2,5-difluorophenylboronic acid (**15**) (1.2 equiv), and $\text{Pd}(\text{PPh}_3)_4$ (0.075 equiv) were placed in 4:1 toluene/EtOH and 2 N Na_2CO_3 (10.0 equiv) was added. The reaction was heated at 85°C for 5 h and then celite was added to the reaction mixture which was then concentrated under reduced pressure. The dry powder was then loaded onto a silica gel column and a gradient of 0–20% EtOAc/hex was used as the eluting solvent to obtain **16** as a yellow solid in 70% yield. Mp $178\text{--}179^{\circ}\text{C}$, LC–MS: $m/z = 337$ ($\text{M}+\text{H}^+$); calcd for $\text{C}_{15}\text{H}_{11}\text{BrF}_2\text{N}_2$: 338 ($\text{M}+\text{H}^+$), ^1H NMR (CDCl_3 , 400 MHz) δ 2.62 (t, $J = 5.8$ Hz, 2H), 3.55–3.62 (m, 2H), 5.25 (br s, 1H), 6.26 (s, 1H), 6.45 (d, $J = 7.9$ Hz, 1H), 6.85–6.95 (m, 1H), 6.96–7.12 (m, 3H).

5.9.24. 4-(2,5-Difluoro-benzyl)-1,2,3,4-tetrahydro-[1,8]naphthyridine (17)

7-Bromo-4-[1-(2,5-difluoro-phenyl)-methylidene]-1,2,3,4-tetrahydro-[1,8]naphthyridine (**16**) was dissolved in methanol and Pd/C was added. The reaction was hydrogenated at atmospheric pressure for 1.5 h. The reaction mixture was then filtered through celite and concentrated under reduced pressure to obtain **17** as a clear colorless oil in quantitative yield. LC–MS: $m/z = 261$ ($\text{M}+\text{H}^+$); calcd for $\text{C}_{15}\text{H}_{11}\text{F}_2\text{N}_2$: 261 ($\text{M}+\text{H}^+$), ^1H NMR (MeOH- d_4 , 400 MHz) δ 1.68–1.86 (m, 2H), 2.80 (dd, $J = 9.0$ Hz, 13.3 Hz, 1H), 2.96 (dd, $J = 10.0$ Hz, 13.3 Hz, 1H), 3.02–3.12 (m, 1H), 3.34–3.41 (m, 1H), 3.46–3.55 (m, 1H), 6.44 (dd, $J = 5.2$ Hz, 7.2 Hz, 1H), 6.93–7.03 (m, 2H), 7.03–7.11 (m, 2H), 7.72 (dd, $J = 1.0$ Hz, 5.0 Hz, 1H).

5.9.25. 6-Bromo-4-(2,5-difluoro-benzyl)-1,2,3,4-tetrahydro-[1,8] naphthyridine (18)

4-(2,5-Difluoro-benzyl)-1,2,3,4-tetrahydro-[1,8] naphthyridine (**17**) was dissolved in a 10:1 mixture of $\text{CH}_2\text{Cl}_2/\text{AcOH}$ and NBS (1.2 equiv) was added. The reaction was stirred at rt for 1 h. and was then concentrated under reduced pressure. The residue was purified by silica gel chromatography using a gradient of 0–60% EtOAc/hex as the eluting solvent to obtain **18** as a clear, colorless oil in 30% yield. LC–MS: $m/z = 339$ ($\text{M}+\text{H}^+$); calcd for $\text{C}_{15}\text{H}_{11}\text{BrF}_2\text{N}_2$: 338 ($\text{M}+\text{H}^+$), ^1H NMR (CDCl_3 , 400 MHz) δ 1.66–1.75 (m, 1H), 1.75–1.86 (m, 1H), 2.73 (dd, $J = 9.6$ and 13.4 Hz, 1H), 2.95 (dd, $J = 6.0$ and 13.4 Hz, 1H), 2.99–3.08 (m, 1H), 3.34–3.43 (m, 1H), 3.45–3.55 (m, 1H), 5.22 (br s, 1H), 6.80–6.86 (m, 1H), 6.88–6.96 (m, 1H), 6.98–7.05 (m, 1H), 7.16 (d, $J = 1.9$ Hz, 1H), 7.91 (d, $J = 1.9$ Hz, 1H).

5.9.26. 4-(2,5-Difluoro-benzyl)-6-[6-(4-methyl-piperazin-1-yl)-pyridin-3-yl]-1,2,3,4-tetrahydro-[1,8] naphthyridine (19)

6-Bromo-4-(2,5-difluoro-benzyl)-1,2,3,4-tetrahydro-[1,8]naphthyridine (**18**) (1 equiv), 1-methyl-4-[5-(4,4,5,5-tetramethyl-[1,3,2]dioxaborolan-2-yl)-pyridin-2-yl]-piperazine (1.4 equiv), and $\text{Pd}(\text{PPh}_3)_4$ (0.1 equiv) were placed in a 4:1 mixture of toluene/EtOH and 2 N Na_2CO_3 (4.0 equiv) was added. The reaction was heated at 90°C for 6 h. The reaction mixture was then concentrated under reduced pressure and the residue was taken up in CH_2Cl_2 and washed with water. The organic layer was dried over Na_2SO_4 , filtered, and concentrated under reduced pressure. Purification by silica gel chromatography using a gradient of 0–20% MeOH/ CH_2Cl_2 as the eluting solvent afforded **19** as a yellow foam in 26% yield. LC–MS: $m/z = 436$ ($\text{M}+\text{H}^+$); calcd for $\text{C}_{25}\text{H}_{27}\text{F}_2\text{O}_5$: 436 ($\text{M}+\text{H}^+$), ^1H NMR (CDCl_3 , 400 MHz) δ 1.7–2.0 (m, 2H), 2.37 (s, 3H), 2.55–2.60 (m, 4H), 2.81 (dd, $J = 9.1$ and 13.3 Hz, 1H), 2.98 (dd, $J = 6.4$ and 13.3 Hz, 1H), 3.08–3.18 (m, 1H), 3.40–3.50 (m, 1H), 3.53–3.70 (m, 5H), 5.18 (br s, 1H), 6.68 (d, $J = 8.8$ Hz, 1H), 6.81–6.87 (m, 1H), 6.89–6.96 (m, 1H), 6.98–7.06 (m, 1H), 7.16 (d, $J = 1$ Hz, 1H), 7.50 (dd, $J = 2.5$ and 8.8 Hz, 1H), 8.05 (d, $J = 1$ Hz, 1H), 8.24 (d, $J = 2.5$ Hz, 1H).

5.9.27. 1-(2,5-Dichloro-benzyl)-4-methyl-7-[6-(4-methyl-piperazin-1-yl)-pyridin-3-yl]-1,2,3,4-tetrahydro-pyrido[2,3-b]-pyrazine (20)

1-(2,5-Dichloro-benzyl)-7-iodo-1,2,3,4-tetrahydro-pyrido[2,3-b]pyrazine (**4f**) was dissolved in anhydrous DMF. NaH (1.6 equiv) was added followed by iodomethane (1.4 equiv). The reaction mixture was stirred at rt for 48 h. Concentration of the reaction mixture followed by column chromatography afforded 1-(2,5-dichloro-benzyl)-7-iodo-4-methyl-1,2,3,4-tetrahydro-pyrido[2,3-b]pyrazine as a yellow solid in 56% yield. LC–MS: $m/z = 434$ ($M+H^+$); calcd for $C_{15}H_{14}Cl_2N_3$: 434 ($M+H^+$), 1H NMR ($CDCl_3$, 400 MHz) δ 3.09 (s, 3H), 3.42 (m, 2H), 3.48 (m, 2H), 4.36 (s, 2H), 6.54 (1H, d, $J = 1.8$ Hz), 7.17 (1H, d, $J = 2.3$ Hz), 7.21 (1H, dd, $J = 8.6, 2.5$ Hz), 7.34 (1H, d, $J = 4.3$ Hz), 7.72 (1H, d, $J = 1.8$ Hz). 1-(2,5-Dichloro-benzyl)-7-iodo-4-methyl-1,2,3,4-tetrahydro-pyrido[2,3-b]pyrazine was coupled to 1-methyl-4-[5-(4,4,5,5-tetra-methyl-[1,3,2]dioxaborolan-2-yl)-pyridin-2-yl]-piperazine through general procedure IIIB to afford **20** as a brown solid in 43% yield. LC–MS: $m/z = 483$ ($M+H^+$); calcd for $C_{25}H_{28}Cl_2N_6$: 483 ($M+H^+$), 1H NMR ($CDCl_3$, 400 MHz) δ 2.33 (s, 3H), 2.52 (t, $J = 5.1$ Hz, 4H), 3.16 (s, 3H), 3.53 (m, 8H), 4.45 (s, 2H), 6.45 (d, $J = 1.8$ Hz, 1H), 6.65 (d, $J = 8.8$ Hz, 1H), 7.18 (dd, $J = 8.5, 4.8$ Hz, 1H), 7.25 (d, $J = 2.3$ Hz, 1H), 7.32 (d, $J = 8.3$ Hz, 1H), 7.52 (dd, $J = 8.6, 2.5$ Hz, 1H), 7.75 (d, $J = 1.8$ Hz, 1H), 8.22 (d, $J = 2.5$ Hz, 1H).

Supplementary data

Supplementary data associated with this article can be found, in the online version, at [doi:10.1016/j.bmc.2010.04.087](https://doi.org/10.1016/j.bmc.2010.04.087).

References and notes

- Duyster, J.; Bai, R.; Morris, S. W. *Oncogene* **2001**, *20*, 5623.
- Armitage, J.O. et al., *Cancer: Principles and Practice of Oncology*, 6th edition, **2001**, pp 2256–2316.
- Kutok, J. L.; Aster, J. C. *J. Clin. Oncol.* **2002**, *20*, 3691.
- Falini, B.; Pulford, K.; Pucciarini, A.; Carbone, A.; De Wolf-Peters, C.; Cordell, J.; Fizzotti, M.; Santucci, A.; Pelicci, P.; Pileri, S.; Campo, E.; Ott, G.; Delsol, G.; Mason, D. Y. *Blood* **1999**, *94*, 3509.
- Morris, S. W. *Br. J. Haematol.* **2001**, *113*, 275.
- Kuefer, M. U.; Look, A. T.; Pulford, K.; Behm, F. G.; Pattengale, P. K.; Mason, D. Y.; Morris, S. W. *Blood* **1997**, *90*, 2901.
- Bai, R.; Dieter, P.; Peschel, C.; Morris, S. W.; Duyster, J. *Mol. Cell Biol.* **1998**, *18*, 6951.
- Bai, R.; Ouyang, T.; Miething, C.; Morris, S. W.; Peschel, C.; Duyster, J. *Blood* **2000**, *96*, 4319.
- Ergin, M.; Denning, M. F.; Izban, K. F.; Amin, H. M.; Martinez, R. L.; Saeed, S.; Alkan, S. *Exp. Hematol.* **2001**, *29*, 1082.
- Slupianek, A.; Nieborowska-Skorska, M.; Hoser, G.; Morrione, A.; Majewski, M.; Xue, L.; Morris, S. W.; Wasik, M. A.; Skorski, T. *Cancer Res.* **2001**, *61*, 94.
- Turturro, F.; Arnold, M. D.; Frist, A. Y.; Pulford, K. *Clin. Cancer Res.* **2002**, *8*, 240.
- Lawrence, B.; Perez-Atayde, A.; Hibbard, M. K.; Rubin, B. P.; Cin, P. D.; Pinkus, J. L.; Pinkus, G. S.; Xiao, S.; Yi, E. S.; Fletcher, C. D. M.; Fletcher, J. A. *Am. J. Pathol.* **2000**, *157*, 377.
- Stoica, G. E.; Kuo, A.; Aigner, A.; Sunitha, I.; Souttou, B.; Malerczyk, C.; Caughey, D. J.; Wen, D.; Karavanov, A.; Riegel, A. T.; Wellstein, A. *J. Biol. Chem.* **2001**, *276*, 16772.
- Powers, C.; Aigner, A.; Stoica, G. E.; McDonnell, K.; Wellstein, A. *J. Biol. Chem.* **2002**, *277*, 14153.
- Mentlein, R.; Held-Feindt, J. *J. Neurochem.* **2002**, *83*, 747.
- Mossé, Y. P.; Laudenslager, M.; Longo, L.; Cole, K. A.; Wood, A.; Attiyeh, E. F.; Laquaglia, M. J.; Sennett, R.; Lynch, J. E.; Perri, P.; Laureys, G.; Speleman, F.; Kim, C.; Hou, C.; Hakonarson, H.; Torkamani, A.; Schork, N. J.; Brodeur, G. M.; Tonini, G. P.; Rappaport, E.; Devoto, M.; Maris, J. M. *Nature* **2008**, *455*, 930.
- Soda, M.; Choi, Y. L.; Enomoto, M.; Takada, S.; Yamashita, Y.; Ishikawa, S.; Fujiwara, S.; Watanabe, H.; Kurashina, K.; Hatanaka, H.; Bando, M.; Ohno, S.; Ishikawa, Y.; Aburatani, H.; Niki, T.; Sohara, Y.; Sugiyama, Y.; Mano, H. *Nature* **2007**, *448*, 561.
- Koivunen, J. P.; Mermel, C.; Zejnullahu, K.; Murphy, C.; Lifshits, E.; Holmes, A. J.; Choi, H. G.; Kim, J.; Chiang, D.; Thomas, R.; Lee, J.; Richards, W. G.; Sugarbaker, D. J.; Ducky, C.; Lindeman, N.; Marcoux, J. P.; Engelman, J. A.; Gray, N. S.; Lee, C.; Meyerson, M.; Jaenke, P. A. *Clin. Cancer Res.* **2008**, *14*, 4275.
- Mosse, Y. P.; Wood, A.; Maris, J. M. *Clin. Cancer Res.* **2009**, *15*, 5609.
- Anand, N. K.; Blazey, C. M.; Bowles, O. J.; Bussenius, J.; Costanzo, S.; Curtis, J. K.; Dubenko, L.; Kennedy, A. R.; Khoury, R. G.; Kim, A. I.; Manalo, J. L.; Peto, C. J.; Rice, K. D.; Tsang, T. H. *PCT Int. Appl.* **2005**, WO 2005009389 A2 20050203.
- Li, R.; Xue, L.; Zhu, T.; Jiang, Q.; Cui, X.; Yan, Z.; McGee, D.; Wang, J.; Gantla, V. R.; Pickens, J. C.; McGrath, D.; Chucholowski, A.; Morris, S. W.; Webb, T. R. *J. Med. Chem.* **2006**, *49*, 1006.
- Leahy, J. W.; Lewis, G. L.; Nuss, J. M.; Ridgway, B. H.; Sangalang, J. C. *PCT Int. Appl.* **2005**, WO 2005097765.
- Galkin, A. V.; Melnick, J. S.; Kim, S.; Hood, T. L.; Li, N.; Li, L.; Xia, G.; Steensma, R.; Chopiuk, G.; Wan, Y.; Ding, P.; Liu, Y.; Sun, F.; Schultz, P. G.; Gray, N. S.; Warmuth, M. *PNAS* **2007**, *104*, 270.
- Cui, J. J.; Funk, L. A.; Jia, L.; Kung, P.; Meng, J. J.; Nambu, M. D.; Pairish, M. A.; Shen, H.; Tran-Dube, M. B. *PCT Int. Appl.* **2006**, WO 2006021886.
- Zou, H. Y.; Li, Q.; Lee, J. H.; Arango, M. E.; McDonnell, S. R.; Yamazaki, S.; Koudriakova, T. B.; Alton, G.; Cui, J. J.; Kung, P.; Nambu, M. D.; Los, G.; Bender, S. L.; Mroczkowski, B.; Christensen, J. G. *Cancer Res.* **2007**, *67*, 4408.
- Cui, J. J.; Bhumralkar, D.; Botrous, I.; Chu, J. Y.; Funk, L. A.; Hanau, C. E.; Harris, G. D., Jr.; Jia, L. *PCT Int. Appl.* **2004**, WO 2004076412.
- Christensen, J. G.; Zou, H. Y.; Arango, M. E.; Li, Q.; Lee, J. H.; McDonnell, S. R.; Yamazaki, S.; Alton, G. R.; Mroczkowski, B.; Los, G. *Mol. Cancer Ther.* **2007**, *6*, 3314. Clinical trial data: <http://www.clinicaltrials.gov/ct2/show/NCT00932893>.
- Ghose, A. K.; Herbertz, T.; Pippin, D. A.; Salvino, J. M.; Mallamo, J. P. *J. Med. Chem.* **2008**, *51*, 5149.
- A single DFG-in homology model was built from insulin like growth factor receptor (IGF1R) structures using the kinase domain (1116–1392) of ALK_human sequence (Swiss-Prot entry Q9UM73), and aminopyridine and constrained aminopyridine scaffolds were docked in it using an automated docking method to elucidate their binding modes (Figs. 3 and 4).
- Carroll, F. I.; Lee, J. R.; Navarro, H. A.; Ma, W.; Briedaddy, L. E.; Abraham, P.; Damaj, M. I.; Martin, B. R. *J. Med. Chem.* **2002**, *45*, 4755.
- DaSettimo, A.; Biagi, G.; Primofiore, G.; Ferrarini, P. L.; Livi, O. *Farmaco-Ed. Sci.* **1978**, *33*, 770. Note: the referenced procedure was followed with the exception of the use of Eaton's reagent rather than PPA.
- Takai, K.; Nitta, K.; Utimoto, K. *J. Am. Chem. Soc.* **1986**, *108*, 7408.
- Fabian, M. A.; Biggs, W. H.; Treiber, D. K.; Atteridge, C. E.; Azimioara, M. D.; Benedetti, M. I.G.; Carter, T. A.; Ciceri, P.; Edeen, P. T.; Floyd, M.; Ford, J. M.; Galvin, M.; Gerlach, J. L.; Grotzfeld, R. M.; Herrgard, S.; Insko, D. E.; Insko, M. A.; Lai, A. G.; Lelias, J.; Mehta, S. A.; Milanov, Z. V.; Velasco, A. M.; Wodicka, L. M.; Patel, H. K.; Zarrinkar, P. P.; Lockhart, D. J. *Nat. Biotechnol.* **2005**, *23*, 329.
- Takemura, H.; Kotoku, M.; Yasutake, M.; Shinmyozu, T. *J. Chem. Res.* **2004**, *12*, 834.
- Gunby, R. H.; Ahmed, S.; Sottocornola, R.; Gasser, M.; Redaelli, S., et al. *J. Med. Chem.* **2006**, *49*, 5759.
- Angeles, T. S.; Steffler, C.; Bartlett, B. A.; Hudkins, R. L.; Stephens, R. M.; Kaplan, D. R.; Dionne, C. A. *Anal. Biochem.* **1996**, *236*, 49.
- Rotin, D.; Margolis, B.; Mohammadi, M.; Daly, R. J.; Daum, G.; Li, N.; Fischer, E. H.; Burgess, W. H.; Ullrich, A.; Schlessinger, J. *EMBO J.* **1992**, *11*, 559.